

# Electrochemical Syntheses of Nanomaterials and Small Molecules for Electrolytic Hydrogen Production

Jia-Qi Wei, Xiao-Dong Chen, Shu-Zhou Li\*

(School of Materials Science and Engineering, Nanyang Technological University,  
50 Nanyang Avenue, Singapore, 639798, Singapore)

**Abstract:** Hydrogen is a clean, efficient, renewable energy resource and the most promising alternative to fossil fuels for future carbon-neutral energy supply. Therefore, sustainable hydrogen production is highly attractive and urgently demanded, especially via water electrolysis that has clean, abundant precursors and zero emission. However, current water electrolysis is hindered by the sluggish kinetics and low cost/energy efficiency of both hydrogen evolution reaction (HER) and oxygen evolution reaction (OER). In this regard, electrochemical synthesis offers prospects to raise the efficiency and benefit of water electrolysis by fabricating advanced electrocatalysts and providing more efficient/value-adding co-electrolysis alternatives. It is an eco-friendly and facile fabrication method for materials ranging from molecular to nano scales via electrolysis or other electrochemical operations. In this review, we firstly introduce the basic concepts, design protocols, and typical methods of electrochemical synthesis. Then, we summarize the applications and advances of electrochemical synthesis in the field of electrocatalytic water splitting. We focus on the synthesis of nanostructured electrocatalysts towards more efficient HER, as well as electrochemical oxidation of small molecules to replace OER for more efficient and/or value-adding co-electrolysis with HER. We systematically discuss the relationship between electrochemical synthetic conditions and the product morphology, selectivity to enlighten future explorations. Finally, challenges and perspectives for electrochemical synthesis towards advanced water electrolysis, as well as other energy conversion and storage applications are featured.

**Key words:** electrochemical synthesis; water electrolysis; electrocatalyst; co-electrolysis; organic electrosynthesis; hydrogen evolution reaction

## 1 Introduction

Hydrogen is one of the most promising sustainable fossil-free fuels nowadays to meet the challenges of growing global industries, increasing energy demands, and arising climate changes for its highest gravimetric energy density ( $142.351 \text{ kJ} \cdot \text{g}^{-1}$ ) and clean combustion process (only water produced)<sup>[1-3]</sup>. Although being eco-friendly, over 95% of nowadays hydrogen is generated by reforming of fossil-fuels, which is a costly and  $\text{CO}_2$  emitting process obstructing the sustainable ecology<sup>[4, 5]</sup>. Alternatively, hydrogen evolution via

water electrolysis has attracted great research attentions as a promising sustainable route for its simple, green and abundant precursor (just water)<sup>[5, 6]</sup>, and high compatibility with renewable electricity (wind turbines, photovoltaics, etc.)<sup>[2]</sup>. Nevertheless, there remain many constraints on the journey of water electrolysis hydrogen production towards practical applications. For example, significantly higher energy inputs than the thermodynamic equilibrium are always required due to the insufficient diffusion, activation barrier, poor energy efficiency, etc. in practical cases.

**Cite as:** Wei J Q, Chen X D, Li S Z. Electrochemical synthesis of nanomaterials and small molecules for electrolytic hydrogen production. *J. Electrochem.*, 2022, 28(10): 2214012.

Moreover, while platinum is recognized as the most efficient electrocatalyst for hydrogen evolution reaction (HER)<sup>[7]</sup>, its preciousness and high cost hinder it from large-scale applications, and there remains lacking cost-effective electrocatalysts with high durability and activity to replace noble metals. Therefore, developing advanced catalysts and electrolytic systems is pivotal in this field.

Explorations in water electrolysis have benefited greatly from nanomaterials<sup>[1]</sup>. The large specific surface area, enriched edge/corner active sites, as well as rationally designed composites have greatly boosted the efficiency, durability, and cost-efficiency of HER electrocatalysis. Among various nano synthetic routes, electrochemical synthesis, or electrosynthesis, is a facile, efficient, and green approach<sup>[8-10]</sup>. It applies electrical potentials between conducting electrodes, which drive analytes in the electrolyte to be oxidized/reduced at electrode-electrolyte interfaces to form products. It has many advantages over other chemical and thermochemical approaches, such as that (i) the process is usually green without the need of hazardous chemicals or high energy input; (ii) the reactions are usually facile and can be well controlled by the potential, current, precursor concentration, etc. and therefore well-engineered nanomaterials and composites can be obtained; (iii) nanostructures/heterostructures can directly grow on conductive substrates like carbon and platinum<sup>[11, 12]</sup>. Various nanomaterials of metals, alloys, and metal compounds have been electrochemically synthesized with low costs, novel designs, and superior catalytical performances, which have contributed significantly to water electrolysis both in terms of new catalyst development and mechanism investigation.

Despite great efforts in developing advanced electrocatalysts towards practical HER, the overall productivity of water electrolysis is also governed by the anodic oxidation. Conventional water electrolysis has oxygen evolution reaction (OER) as the anodic reaction, which usually has higher activation barrier and more sluggish kinetics than HER<sup>[13, 14]</sup>. Moreover, the O<sub>2</sub> generated by OER is less valuable and may con-

taminate H<sub>2</sub> as a gas impurity, leading to low overall efficiency and profit for hydrogen production<sup>[15]</sup>. The mixture of H<sub>2</sub>, O<sub>2</sub>, and catalysts may also generate active oxygen species to degrade the electrolysis device. These factors hold the back of water electrolysis towards real applications. In view of this, electrochemical synthesis also provides novel solutions by introducing other anodic electrochemical oxidations to replace OER and form hybrid co-electrolysis systems with HER (also called chemical-assisted HER)<sup>[13, 15, 16]</sup>. Indeed, in addition to nano fabrications, electrochemical synthesis can also be extended to small molecules via direct redox reactions at electrode/electrolyte interfaces<sup>[17]</sup>. Various anodic electrochemical syntheses like the oxidation of hydrazine and alcohols, which have highly water soluble precursors, lower potentials and faster kinetics than OER, no competition with HER, inhibits gases crossover, and/or form value-added products, have been employed to replace OER, forming redox couples with HER. Such hybrid electrochemical synthetic systems can therefore produce H<sub>2</sub> in greener and more efficient ways with other possible economically viable products<sup>[18, 19]</sup>.

In short, electrochemical synthesis has played an important role in electrolytic hydrogen evolution and is promising to contribute further. Herein, we summarize explorations in electrochemical synthesis associated with electrolytic hydrogen generation. We firstly introduce fundamental aspects, design protocols, and typical methods of electrochemical synthesis. Then, we summarize the electrochemically synthesized electrocatalysts for HER (Figure 1), which include platinum group metals (PGMs), transition metals (TMs), alloys, and transition metal compounds including oxides (TMOs), dichalcogenides (TMDs), phosphides (TMPs), carbides (TMCs), and others. After that, various electrochemical oxidations of small molecules are discussed as alternatives to OER towards more efficient and/or value-adding co-electrolytic hydrogen production, including the alcohol oxidations (AORs), carbohydrate oxidations (CHOORs), amine oxidations, aldehyde oxidations (AhORs), water oxidation (WOR), and hydrazine oxidation (HzOR),

urea oxidation (UOR), ammonia oxidation (AmOR). We focus on electrochemical synthetic methodologies and parameters, including the system design, the reaction potential, current, substrate, electrolyte composition and concentration, electrocatalysts, etc. with tailored outcomes. This is complementary to previous reviews in this field, which rather focused on electrochemical synthesis of nanomaterials itself or for other applications<sup>[9, 11, 12]</sup>, or electrocatalytic organic synthesis associated with hydrogen production<sup>[13, 15, 19]</sup>. Lastly, we also discuss the challenges and perspectives in electrochemical synthesis towards more efficient hydrogen generation as well as other energy conversion and storage applications. The electrochemical synthetic strategies and examples summarized herein, therefore, provide guidance for future explorations.

## 2 Basic Aspects and Protocols of Electrochemical Synthesis

### 2.1 Fundamental Aspects of Electrochemical Synthesis

Electrochemical synthesis, also called electrosynthesis, is performed by applying electricity between two or more electrodes separated by an electrolyte, therefore inducing diffusion of analytes towards the electrode surface and oxidizing/reducing them at the interfaces. It has a long history since 1800, when the first voltaic pile and water electrolysis was created—indeed, water electrolysis is also a form of electrochemical synthesis of  $H_2$  and  $O_2$ <sup>[8]</sup>. A basic electrochemical synthesis system consists of a cathode and an anode, merged in an ionically conducting electrolyte and connected electrically to an external power supply. During an electrochemical synthesis, the anode/cathode is positively/negatively charged by the external power source, attracting oppositely charged species in the electrolyte to form electrical double-layers on the electrode surfaces. Once the redox potential of the analyte is reached, the anode extracts electrons from the interfacial species and oxidizes it, analogous to an oxidizing agent, while the cathode provides electrons to the species and reduces it, similar to a reducing agent. The key parameters governing an electrochemical synthesis are therefore the

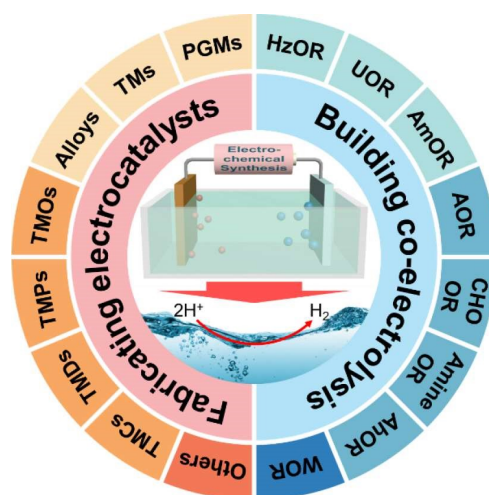


**Figure 1** Scheme of the electrochemical synthesis associated with water electrolysis hydrogen production. The left side lists electrochemical syntheses of HER electrocatalysts, including PGMs, TMs, alloys, TMOs, TMPs, TMDs, TMCs, and others. The right side summarizes electrochemical oxidations of small molecules to form co-electrolysis with HER, including HzOR, UOR, AmOR, AORs, CHOORs, amine ORs, AhORs, and WOR. (color on line)

electrifying method, electrolyte concentration and composition, and electrode surface. The reaction temperature, pressure, and atmosphere also show influences on the reaction.

With the abovementioned characteristics, electrochemical synthesis has several advantages over chemical and thermochemical routes, which are: (i) more eco-friendly without the needs for oxidants/reductants as well as reduced/oxidized wastes; (ii) energy saving with milder reaction temperatures and pressures; (iii) highly engineerable reaction processes and parameters, and therefore high controllability/selectivity over products; (iv) easily scaled up with greater potentials for practical applications. Also, it has some drawbacks, such as that (i) complete electrochemical devices are required, which can be expensive and hard to maintain; (ii) supporting electrolytes can be required and bring additional cost; (iii) ion exchange membranes can be required to divide cells with metal catalysts and/or dual electrolytes/products; (iv) reactions are limited on conductive interfaces.

## 2.2 Constructing an Electrochemical Cell for Synthesis

A successful electrochemical synthesis relies on the proper design of the electrochemical system. As shown in Figure 2a, an electrochemical synthetic system usually consists of an electrolyte tank, a power supply, a working electrode (WE) to carry the desired reaction, a counter electrode (CE) to close the electric circuit, an electrolyte to ionically conduct electricity, and sometimes also contains a reference electrode (RE) to steadily monitor the potential change, a separator to separate the cathode and anode, etc. The electrolyte can be further disassembled into solvents and solutes (analytes, supporting electrolytes, additives). The most often used electrochemical cell setups are the two- and three-electrode setups. The two-electrode setup is the most basic form of an electrochemical cell, in which the energy is directly applied between the WE and the CE. The electrodes balance their potentials automatically to meet the redox reaction, and the overall potential difference meets the applied potential. Contrarily, in three-electrode setups, the potential is applied to the WE, which is referred to the constant potential of the RE. The CE's potential is adjusted such that the WE-RE potential difference meets the desired input and the electrochemical circuit is closed. As such, three-electrode setups demonstrate the WE's efficiency rather than the overall cell efficiency, while two-electrode tests can determine the actual efficiency of an electrochem-

ical device.

As a part of the interfacial system, the electrode material, which conducts electricity and carries redox reactions, undoubtedly plays a key role in electrochemical synthesis. As mentioned above, the nature of electrochemical synthesis requires electrodes to be conductive and as the substrate of reactions. For a particular electrochemical system, the electrode needs to be electrochemically and chemically stable within the operation potential window. The frequently used electrodes include platinum and carbon as both the cathode and anode, mercury, lead, and silver for the cathode, as well as nickel, magnesium, aluminium, iron, and zinc as the anode<sup>[20]</sup>. Each of the electrodes has its pros and cons, which have been well reviewed elsewhere<sup>[21]</sup>. Additionally, various catalysts can be loaded on the conducting electrode surface to promote more efficient redox reactions. Choosing the right material and even the right surface is critical for the success of an electrochemical synthesis.

Another dominating component of electrochemical synthesis is the electrolyte. Carrying on electrochemical reactions at the interface, several factors need to be considered to choose appropriate electrolytes: (i) the proton activity, which influences the reduction of radical anions and proton elimination from oxidation-generated radical cations; (ii) the electrochemical window, which should be larger than the operational potential range of an electrochemical synthetic system; (iii) the dielectric constant, which controls the elec-

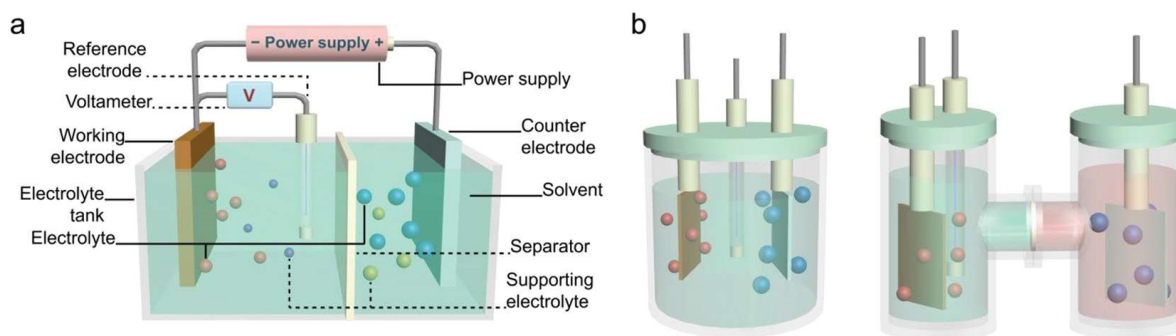


**Figure 2** a) Scheme of an electrochemical cell consisting (solid lines) a tank, a WE, a CE, a power supply, an electrolyte, and possibly (dash lines) a RE, an additional voltmeter, a separator, and supporting electrolytes. b) Scheme of a typical non-divided cell (left) and a divided “H” cell (right). (color on line)

trolyte dissociation and thus influences its resistance. The main solvents nowadays include: (i) water, which is most widely involved in various inorganic systems but poorly dissolves organic species; (ii) alcoholic solvents, which are good at conducting anodic oxidation with themselves being reduced at the cathode; (iii) amine-based solvents, which have been used usually in reduction and for highly basic species; (iv) acetonitrile (ACN), which has been popular for all types of reactions for its wide electrochemical window and high conductivity; (v) N,N-di-methylformamide (DMF) and dimethyl sulfoxide (DMSO), which have good solubility to many organic and inorganic compounds. There are also many other solvents with special characters being used for electrochemical synthesis, which have been summarized elsewhere<sup>[8]</sup>.

During syntheses, conductive analytes in the electrolyte could be consumed as precursors. Therefore, supporting electrolytes should be added as charge carriers<sup>[22]</sup>. The choice of supporting electrolytes depends on their solubility, interactions in solvents, and compatibility with the redox reaction. Perchlorate ( $\text{ClO}_4^-$ ), tetrafluoroborate ( $\text{BF}_4^-$ ), hexafluorophosphate ( $\text{PF}_6^-$ ), and trifluoromethanesulfonate ( $\text{CF}_3\text{SO}_3^-$ ) anions are good candidates for supporting anions for their high oxidization resistance, while the latter three offer additional high stability. Lithium ( $\text{Li}^+$ ) and sodium ( $\text{Na}^+$ ) cations are stable and hardly reduced, thus working well as supporting cations. Nevertheless, they may co-precipitate with the synthetic products on the electrode surface, and sodium salts are rarely soluble in organic solvents. Metal-free choices can be quaternary ammonium cations ( $\text{NR}^{4+}$ , R could be Me, Et, Bu, etc.), which also facilitate the dissolution of organic species in water.

Depending on the reaction to be performed, and the need to separate electrolytes and analytes, electrochemical synthesis can be carried out in a unified cell or divided cell. As shown in Figure 2b (left), in an undivided cell, the electrolyte can move freely to the cathode or the anode, which is facile and easily adapted for electrochemical synthesis with only one stable target. However, undivided cell fails in cases

that both oxidation and reduction proceed with desired products (co-electrolysis), or the analytes, products, intermediates, etc. can undergo further undesired reactions with each other or the electrodes. Under such conditions, it is necessary to divide the cell with a diaphragm so that the catholyte and anolyte do not meet each other. Conventionally, such divided cells often adopt a “H” shape and are referred to as the “H-cell” (Figure 2b, right).

Based on the desired product, electrochemical synthesis can happen on either the cathode, anode, or both, which influences the construction of the synthetic system. During electrifying, the anode is electron-lacking and tends to gain electron from reactants and oxidize them. Electrochemical syntheses of metal oxides, nitrides, etc. with higher valance state from pure metal, lower valance metal compounds, etc. happen at the anode<sup>[12]</sup>. Oxidations of small molecules towards more value-adding products like AORs, CHOORs, and WOR also take place here<sup>[16, 23]</sup>. Contrarily, the cathode is electron-rich and offers electron to reactants to reduce them. Therefore, electrochemical reduction towards pure metals, metal compounds, hydrogen, as well as organic compounds, etc. with lower valances are done on the cathode<sup>[9, 17, 24, 25]</sup>. Depending on the electrode of target, the counter-reaction on the opposite electrode may originate from the solvent, sacrificial agent, or other additives in the electrolyte that should have no pollutant to the product. It is also possible to have parallel electrochemical syntheses at both electrodes with desired products, or even combinations of reactants at both electrodes into single products<sup>[18]</sup>. This often takes place for the synthesis of molecular products and is referred to as co-electrolysis. It is worth mentioning that, in electrochemical exfoliation introduced later, due to the different definitions of cathode and anode, that the reaction happens is in the opposite way: the cathode attracts anions and intercalates them to exfoliate itself, while the anode plays with cations.

### 2.3 Electrical Operations for Synthesis and Hydrogen Evolution Analysis

With appropriate synthetic systems, various electro-

analytical methods can be applied to perform the synthesis or investigate synthetic mechanisms. Based on the electrical parameter under control, most of the electroanalytical methods can be categorized into either potentiostatic or galvanostatic.

Potentiostatic operations like cyclic voltammetry (CV) and chronoamperometry apply controlled potentials to cells during electrochemical analyses. CV tests apply a constant potential ramp and record the current response (Figure 3a). Initially, it is merely capacitive since no charge transfer happens. Once the analyte's redox potential is reached, it is reduced/oxidized, and the current peak is observed. After that, the current drops, with which reactions still happen but decrease due to the depletion of reactants near the interface. When the potential is reversely swept, a corresponding redox peak could be captured if the redox product is stable and remains to be converted back. Due to the requirement of more complicated setup and longer reaction time, CV is less used in real electrochemical synthesis. Nevertheless, the informative spectrum allows one to acquire the reaction potential, overpotential, kinetics, reversibility, route, etc. and thus understand reactions electrochemically<sup>[26]</sup>. Therefore, CV is seldom absent in analysing synthetic mechanisms or hydrogen evolution performances, especially for those of organic electrochemical syntheses with multiple products. During analyses, the sweep is often one way from smaller to larger potentials, which is therefore called linear scanning voltammetry (LSV). LSV is basically the early parts of CV including the capacitive initiative and sharply raised redox park (Figure 3b).

As shown in Figure 3c, chronoamperometry is to

fix the electrochemical system at certain potentials and records the time-dependent response of current. It requires simpler electrical functionality and thus equipment than CV, and is intensively employed in electrochemical synthesis, especially in electrodeposition and small molecule syntheses with multiple potential steps and products. Moreover, the  $I-t$  curve contains reaction kinetics information of electrochemical synthetic processes, especially for analyte adsorption, which can be mathematically extracted. Therefore, it is often combined with CV, etc. for electrochemical analyses<sup>[27]</sup>.

If the cell current is controlled, the operation is called galvanostatic. Galvanostatic charge/discharge (GCD) is a typical method by applying a constant current to the electrochemical cell and measuring the potential change over time (Figure 3d). During GCD, the potential changes with time due to the formation of an electrical double-layer. When the potential of a redox reaction is reached, the potential is flattened into a plateau and the redox reaction takes place. As the reaction proceeds towards the equilibrium, the activity decreases and the potential drifts to the second redox plateau. During GCD processes, the current can be tailored to control the reaction rate and thus the product particle size, morphology, etc<sup>[28]</sup>. Therefore, it is often used in electrochemical syntheses with sole products, or nanomaterial syntheses that structure, morphology, and/or size matters. It is also used in electrochemical exfoliation, modification, etc.

In practical, electrochemical synthesis can be performed either potentiostatically or galvanostatically. While real systems are usually multi-step with side reactions, controlling the potential leads to full control

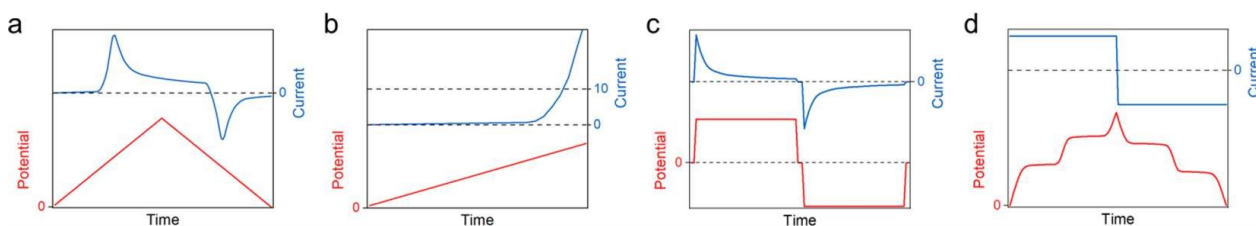


**Figure 3** Typical potential/current-time curves for a) cyclic voltammetry, b) linear scanning voltammetry, c) chronoamperometry, and (d) galvanostatic charge/discharge test. (color on line)

of the synthetic reaction and therefore higher selectivity. Nevertheless, this also leads to longer reaction time and more complicated setup. Contrarily, galvanostatic methods are faster and simpler, but may lead to a mixture of multiple products and therefore lower selectivity.

## 2.4 Typical Electrochemical Synthesis Methods

Being properly organized as abovementioned, electrochemical syntheses are usually conducted using four typical methods: direct electrochemical oxidation/reduction, electrodeposition, electrochemical exfoliation, and electrochemical modification.

Direct electrochemical oxidation/reduction is the most basic form of electrochemical synthesis. It involves oxidation and/or reduction of reactants from the electrolyte or on the electrode surface, directly at the electrode/electrolyte interface. The product, either in gas phase released from the cell, in liquid phase mixed in the electrolyte, or in solid phase precipitated into the electrolyte/on to the electrode, is collected and purified after the reaction. This simple method is usually used for molecular materials synthesis, of which the product usually adopts gaseous or liquid format<sup>[17]</sup>.

If the product is in the form of a thin film, coating, or nano-decoration on the electrode, the method is usually referred to as electrodeposition, or electroplating<sup>[29-31]</sup>. It has a long history over two centuries that originally used to apply metallic coatings on conductive surfaces<sup>[32]</sup>. Nowadays, electrodeposition is intensively used to grow metals, ceramics, and even organic coatings on conductive substrates (electrodes) with varying thicknesses, compositions, and nanostructures to build novel catalysts. The substrate of electrodeposition can also be part of the catalyst matrix to form advanced composites. During electrodeposition, the reaction rate and the product size, nanostructure, morphology, density, etc. can be well controlled by tailoring the electrifying method, deposition current, potential, electrolyte, additive, as well as temperature, pressure, etc. with the interplay of many physiochemical factors like crystallography and

mass transport behind.

In addition to those direct methods, electrochemical syntheses can also be performed combining with other electrochemical systems. Electrochemical exfoliation is a typical synthetic method to fabricate layered nanosheets<sup>[33-35]</sup>. It is performed by electrochemically introducing foreign species, often metallic cations and various anions, into the interlayer space of layered materials, which causes structural expansion and loosens the interlayer binding, thus can exfoliate them into single- or few-layer nanosheets. The intercalation is usually performed with a battery-like setup, and both conductive and nonconductive layered nanomaterials such as graphene<sup>[33]</sup>, transition metal compounds<sup>[36]</sup>, phosphorus<sup>[37]</sup>, etc. can be exfoliated. The thickness, defect density, etc. can be controlled by tailoring reaction parameters like intercalation species, potential, current, time, electrolyte composition, exfoliation method, etc.

Apart from new material fabrication, electrochemical methods have also been intensively used to modify the property of existing materials<sup>[38]</sup>. Electrochemical modification is to regulate the physical and chemical properties of materials via electrochemical treatments, usually in an electrochemical device (battery, etc.)-like setup. Compared to other methods, it has milder processes, easier and more precise control, as well as lower chemical and environmental hazards. Various electrochemical modification approaches like intercalation (like exfoliation) and conversion have been developed, which can tune the electronic structure, crystal phase and crystallinity, lattice strain, size and boundary, etc. of the material.

## 3 Electrochemical Synthesis of Nanomaterials for Hydrogen Evolution Reaction

### 3.1 Metallic Electrocatalysts

As demonstrated by the volcano plot and many research works, Pt group metals (Pt, Pd, Ru, Ir, Rh) have superior HER catalysing performance with much smaller hydrogen adsorption energy compared to most other materials<sup>[1, 3]</sup>. Considering the high cost of these



metals and the interfacial nature of water electrolysis, thin films, nanoparticles, etc. with large surface area-to-volume ratios are desired. Such nanomaterials can be readily fabricated via electrodeposition<sup>[39-41]</sup>. Compared to traditional electrodeposition in cyanide-based toxic electrolytes, water and deep eutectic solvents that are greener, nontoxic, electrochemically more conductive, and more soluble to metals have been good alternatives for the electrodeposition of metallic catalysts<sup>[42-45]</sup>. As shown in Figure 4, Bard's group electrodeposited Pt clusters on bismuth ultramicroelectrode using  $\text{fmol} \cdot \text{L}^{-1}$ -level  $\text{PtCl}_6^{2-}$  aqueous electrolytes<sup>[45]</sup>. The resulted Pt clusters show sizes of up to 9 atoms, which are precisely controlled by the plating pulse of suitable duration and the low precursor concentration with limited diffusion rate. Once deposited, Pt clusters clearly show activity towards HER, which is not seen with bare ultramicroelectrode.

The size, shape, and facet of noble metals, which are the three key factors influencing their HER activity, can be well controlled in electrochemical synthesis by adjusting parameters like the charging protocol, electrolyte composition and concentration, and additive<sup>[46-55]</sup>. For example, Bard's group electrodeposited Pt single atom, clusters with one to five atoms, and nanoparticles up to  $\sim 10$  nm radius on ultramicroelectrodes by controlling the electrolyte concentration and deposition time (Figure 5a-c)<sup>[46]</sup>. The HER kinetics increases as the Pt size increases from a

single atom to  $\sim 4$  nm cluster and then reaches a plateau. This is due to a kinetic size effect changing the  $\text{H}^+$  adsorption energy, which approaches the bulk performance at larger enough cluster sizes (Figure 5d)<sup>[6, 56]</sup>. Other nanostructures like porous Pt, Pt nanopines, etc. have also been achieved by controlling the template, ionic concentration, and current density during electrolysis (Figure 5e, f)<sup>[47, 57, 58]</sup>. Taking the porous Pt film developed by Schmidt's group as an example, the process involves a two-step reduction of  $\text{PtCl}_4$  during electrodeposition, while simultaneous hydrogen evolution causes the porosity development<sup>[47]</sup>. The pore size and conductivity of the porous Pt are controllable by tailoring the deposition potential and additive concentration (Figure 5g-n). Kiani et al. introduced CO into the reduction of Pt ion to metallic Pt, leading to significantly reduced deposition amount but much improved mass activity with 31 mV overpotential (the additional potential than the equilibrium required to drive a reaction) and  $35 \text{ mV} \cdot \text{dec}^{-1}$  Tafel slope (correlation factor between the reaction kinetic and the overpotential) at  $10 \text{ mA} \cdot \text{cm}^{-2}$ <sup>[48]</sup>. The superior activity than commercial Pt/C (27.8 mV at 20wt%Pt) is likely induced by the enriched Pt(111) surface in the product with maximum tolerance against CO absorption.

Along the way of catalysts' nano dispersion, various supporting materials also contribute significantly during both the electrochemical synthesis and the electrocatalysis. They offer electrically conducting

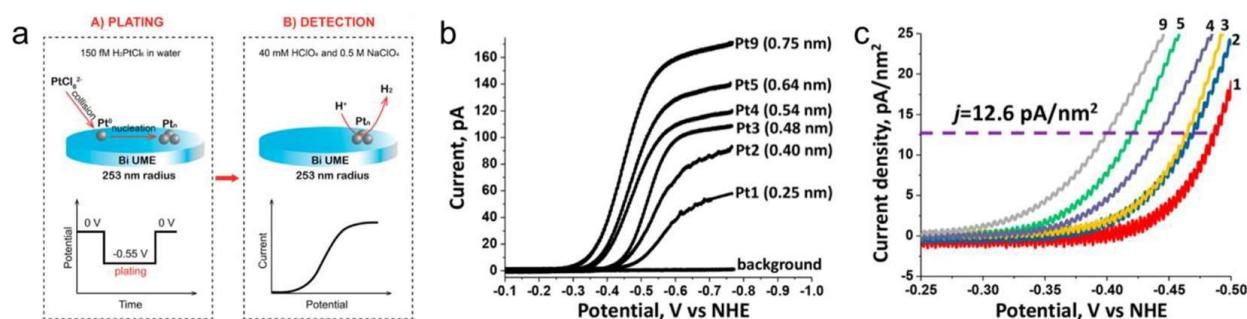


**Figure 4** a) Scheme of the electrodeposition and HER analysis protocols for Pt clusters. b) LSV plots for Pt clusters under  $50 \text{ mV} \cdot \text{s}^{-1}$  in a deaerated  $40 \text{ mmol} \cdot \text{L}^{-1} \text{HClO}_4$  and  $0.5 \text{ mol} \cdot \text{L}^{-1} \text{NaClO}_4$ , with which the cluster size can be estimated. c) Zoomed region in (b) at a current density of  $12.6 \text{ pA} \cdot \text{nm}^{-2}$ , which demonstrated the increasing HER activity of Pt clusters with sizes. Reproduced with permission from Ref. 45. Copyright 2017 American Chemical Society. (color on line)



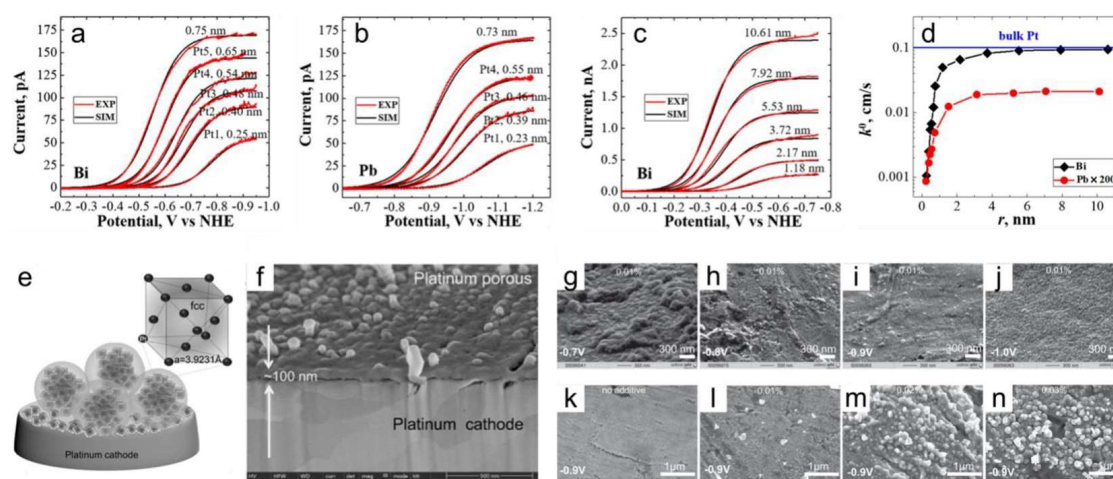


**Figure 5** a-c) The HER volammograms of Pt clusters (a, b) and nanoparticles (b) on ultramicroelectrodes of Bi (a, c) and Pb (b). The red curves represent experimental results, while the black ones are simulated results. d) The HER kinetic constant as a function of the Pt radius and type of substrate. The blue line represents the one for bulk Pt. The Pb one is magnified 200 times for comparison. Reproduced with permission from Ref. 46. Copyright 2019 American Chemical Society. e-f) Scheme (e) and SEM image (f) of porous Pt layer electrochemically grown on the Pt cathode. g-j) SEM images of porous Pt obtained from the same electrolyte under different potentials. k-n) SEM images of porous Pt obtained under the same potential at different additive concentrations. Reproduced with permission from Ref. 47. Copyright 2021 Springer Nature. (color on line)

connections to link nanosized catalysts to the external circuit, and high surface area to enlarge the catalyzing interface. Currently, the most widely used supporting materials are various carbon materials such as carbon nanotube<sup>[59, 60]</sup>, graphene<sup>[61, 62]</sup>, and activated carbons<sup>[63]</sup>, for their high electrical conductance and specific surface area. For example, Laasonen et al. electrochemically deposited sub-nano cluster Pt on the surface of SWCNT, achieving similar HER performance to commercial Pt/C with more than 60-fold heavier loading (Figure 6a-d)<sup>[59]</sup>. The curved structure of thin SWCNT greatly stabilizes Pt clusters and therefore contributes to the atomic-scale dispersion. Apart from carbon materials, other substrates like metal foam,  $\text{Ni}_3\text{N}$ <sup>[64]</sup>, polypyrrole (PPy)<sup>[65]</sup>, poly(3,4-ethylenedioxythiophene) (PEDOT)<sup>[66]</sup>, have also been attempted in electrochemical synthesis. In addition to high electrical conductance, these substrates also provide other functions like facilitating water dissociation and/or hydrogen intermediate generation towards advanced HER (Figure 6e-h). It is also possible to be substrate-less and electrochemically generated metal nanoparticles at liquid-liquid interfaces to catalyze hy-

drogen evolution *in situ*<sup>[67, 68]</sup>. By constructing a water/1,2-dichloroethane immiscible system, Girault's group has *in situ* synthesized Pt and Pd nanoparticles at the interface by electroreduction of  $\text{PtCl}_4^{2-}$  or  $\text{PdCl}_4^{2-}$  with DMFC as the electron donor under the interfacial Galvani potential difference<sup>[67]</sup>. The resulted nanoparticles are adsorbed at the interface and show catalytic properties with a 0.55 V positive polarization.

Apart from being used solely, electrochemical synthesis may also integrate with other methods to achieve novel and/or hierarchical structures<sup>[69-71]</sup>. For example, Qin's lab electrodeposited Pt on solvothermally pre-synthesized  $\text{WO}_3$ -on-Cu foam ( $\text{WO}_3$ @CF)<sup>[71]</sup>. The process uses bulk Pt as the precursor and utilizes its oxidation, dissolution during acidic OER and reduction during HER, resulting in a PtCu alloy on  $\text{WO}_3$ @CF nanostructure with well-controlled Pt loading (Figure 7a-c). The PtCu/ $\text{WO}_3$ @CF electrocatalyst shows ultrahigh Pt mass activities of 1.35 and 10.86  $\text{A} \cdot \text{mg}^{-1}_{\text{Pt}}$  at 20 and 100 mV overpotentials, respectively, which are 27 and 13 times higher than those of commercial Pt/C catalysts, respectively (Figure 7d-f). The origin of such excellent performance is the enhanced reactivity

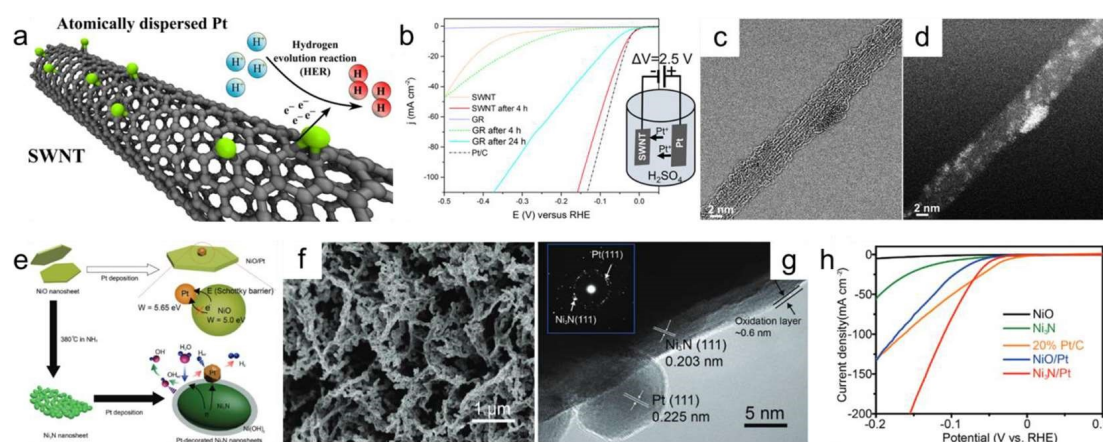


**Figure 6** a) Schematic representation of the atomically dispersed Pt on curved CNT surface catalysing the HER. b) Polarization curves of CNT, graphite, their activated counter parts, and commercial Pt/C, in a 0.5 mol·L<sup>-1</sup> H<sub>2</sub>SO<sub>4</sub> solution with Pt foil as the counter electrode. The inset shows the activation setup. c-d) Bright field (c) and corresponding high-angle annular dark-field (HAADF) (d) images of a CNT bundle after activation. Reproduced with permission from Ref. 59. Copyright 2017 American Chemical Society. e) Scheme showing the electrodeposition of Pt on Ni<sub>3</sub>N and the synergistic HER mechanisms of Ni<sub>3</sub>N/Pt. f-g) SEM (f) and HRTEM (g) images of Ni<sub>3</sub>N/Pt. Inset in (g) is the selected area electron diffraction (SAED) patterns of Ni<sub>3</sub>N/Pt. h) HER activity of Ni<sub>3</sub>N/Pt in 1 mol·L<sup>-1</sup> KOH compared with various control groups. Reproduced with permission from Ref. 64. Copyright 2017 John Wiley and Sons. (color on line)

and number of active sites by the hollow sphere structure, as well as the hydrogen spillover effect by the synergy between WO<sub>3</sub> and Pt. Xiao et al. utilized the electrolysis method to produce Pt nanoparticles and carbon quantum dots (CQDs) simultaneously in a double Pt wire setup in propylene carbonate-based electrolytes and merged them onto carbon nanotube (CNT) in subsequent solvothermal treatment<sup>[70]</sup>. The two-step synthesized Pt-CDQs/CNT demonstrates 35.3 mV overpotential at 10 mA·cm<sup>-2</sup> for HER, comparable to commercial Pt/C catalyst even at much lower loading (0.81wt%). By tuning the electrolysis potential, type of supporting electrolyte, etc. the amount and size of Pt NPs and CQDs can be defined.

To date, noble metals are still the most effective HER electrocatalysts with low overpotentials and fast kinetics. However, their low abundance and high cost prevent them from being commercially applied even under reduced overall usage with small nanoparticles. To this end, alloying engineering to enhance the catalytic performance and further minimize the noble metal usage has been intensively investigated as a

promising alternative strategy<sup>[72-74]</sup>. Electrochemical synthesis has also contributed significantly to this field. For example, Pellicer's group developed Fe-Pt mesoporous thin films through micelle-assisted electrodeposition, which have tailored roughness and Fe content with different metal substrates (Figure 8a-c)<sup>[73]</sup>. Ultra-smooth surface with evenly distributed mesoporous and high Fe content (21wt%) can be obtained on Au substrate, which shows -7 mV overpotential at 10 mA·cm<sup>-2</sup> in 1.0 mol·L<sup>-1</sup> KOH alkaline electrolyzer. Various transition metal-based alloys can also be electrochemically fabricated with advanced HER performances<sup>[75-78]</sup>. Chung's group electrodeposited Au<sub>x</sub>Cu<sub>100-x</sub> foams with controlled ratios by controlling the precursor concentration, and then galvanically displaced some of the Cu atoms<sup>[76]</sup>. During the process, the Au serves as a buffer to release the mechanical stress and prevent the detachment. Therefore, the tailorable Pt@Au<sub>x</sub>Cu<sub>100-x</sub> electrocatalysts show advanced catalytic performance in an alkaline electrolyzer. Dick et al. developed a generalized nanodroplet-mediated electrodeposition method to synthesize alloys of up to 8 metallic elements (high-entropy metallic glasses),

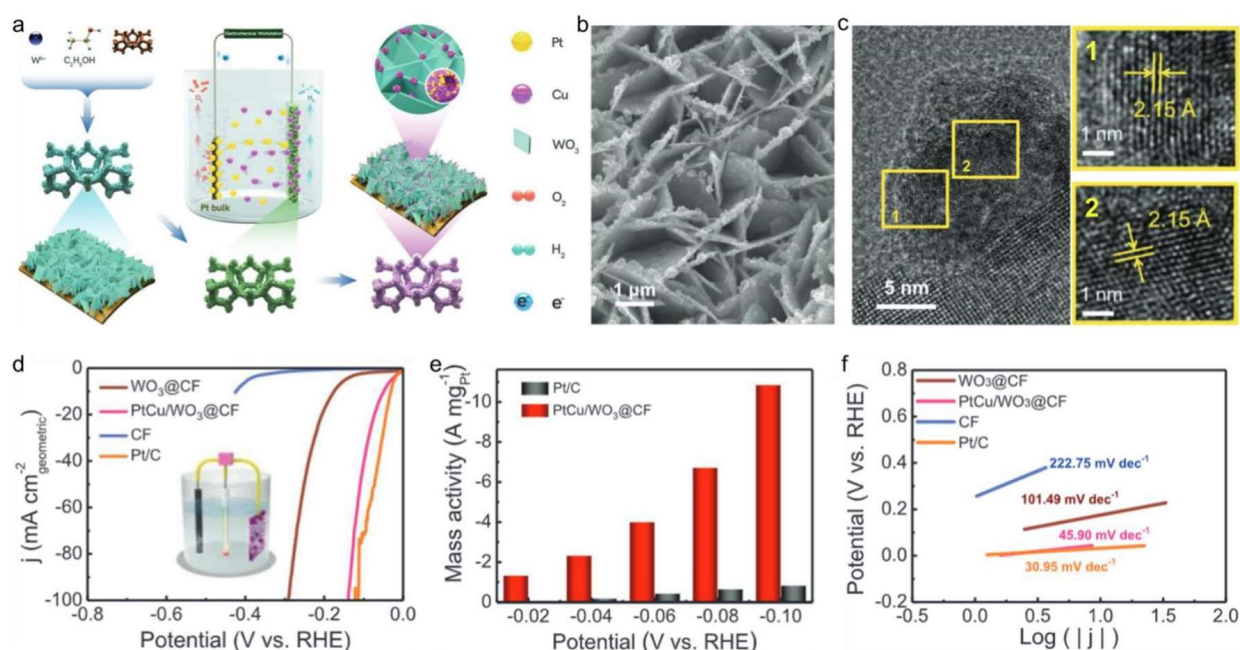


**Figure 7** a) Scheme of the solvothermal-electrodeposition process for preparing PtCu/WO<sub>3</sub>@CF. b-c) representative SEM (b) and TEM (c) images of PtCu/WO<sub>3</sub>@CF. The zoomed images 1 and 2 (right) in (c) are the enlarged feature in the yellow squares 1 and 2 (left). d) LSV plots of PtCu/WO<sub>3</sub>@CF and other control catalysts for HER. e) Pt mass-specific current density graphs of PtCu/WO<sub>3</sub>@CF and commercial Pt/C at different potentials. f) Tafel plots of PtCu/WO<sub>3</sub>@CF and other control catalysts from the LSV result. Reproduced with permission from Ref. 71. Copyright 2022 John Wiley and Sons. (color on line)

which provides tunable water electrolysis catalysing performance based on the properties of compositional metals (Figure 8d-g)<sup>[79]</sup>. By tuning the precursor concentration in nanodroplet, precise control of the alloy stoichiometry can be achieved, with which the CoFe-LaNiPt alloy demonstrates superior water electrolysis performance.

In addition to alloy catalysts, nonprecious metals such as Ni<sup>[28, 80, 81]</sup>, Co<sup>[82]</sup>, as well as their alloys<sup>[83-85]</sup>, have been attempted as even cheaper alternatives and electrochemical synthesis has also been utilized for preparing them<sup>[25]</sup>. For example, Lee et al. prepared Ni nanowires by porous alumina templated galvanic electrodeposition, which has a high aspect ratio of 100 and large electrocatalytic active Ni(111) surface, therefore delivering good catalytic performance<sup>[80]</sup>. The structure, surface area, and edge facets of the electrodeposited TM are tailorable with the deposition potential, similar to noble metal electrochemical syntheses, therefore adjusting the HER catalytic performances<sup>[28]</sup>.

### 3.2 Metal Compound Electrocatalysts

Another low-cost yet efficient strategy to catalyze HER is to use non-noble metal compound electrocatalysts for their earth abundance, high accessibility, as well as tunable compositions and properties. To date, great breakthroughs have been accomplished in developing transition metal-based compounds for HER catalyzing, including TMOs, TMNs, TMCs, TMDs, TMPs, TMBs, etc. as well as their composites<sup>[1, 86]</sup>. Electrochemical synthesis plays important roles in fabricating and exploring these materials with novel nanostructures and/or mechanisms.

TMOs have been intensively studied and used in electrocatalysis. They are one of the most promising candidates for HER so far, for their cost-efficiency, stability, accessibility, and sustainability. However, their intrinsic low electrical conductivity and the need for a large surface area make them usually proceed with small nanostructures, conductive dopants, and/or integration with conductive substrates. This is especially suitable for using electrochemical synthesis.



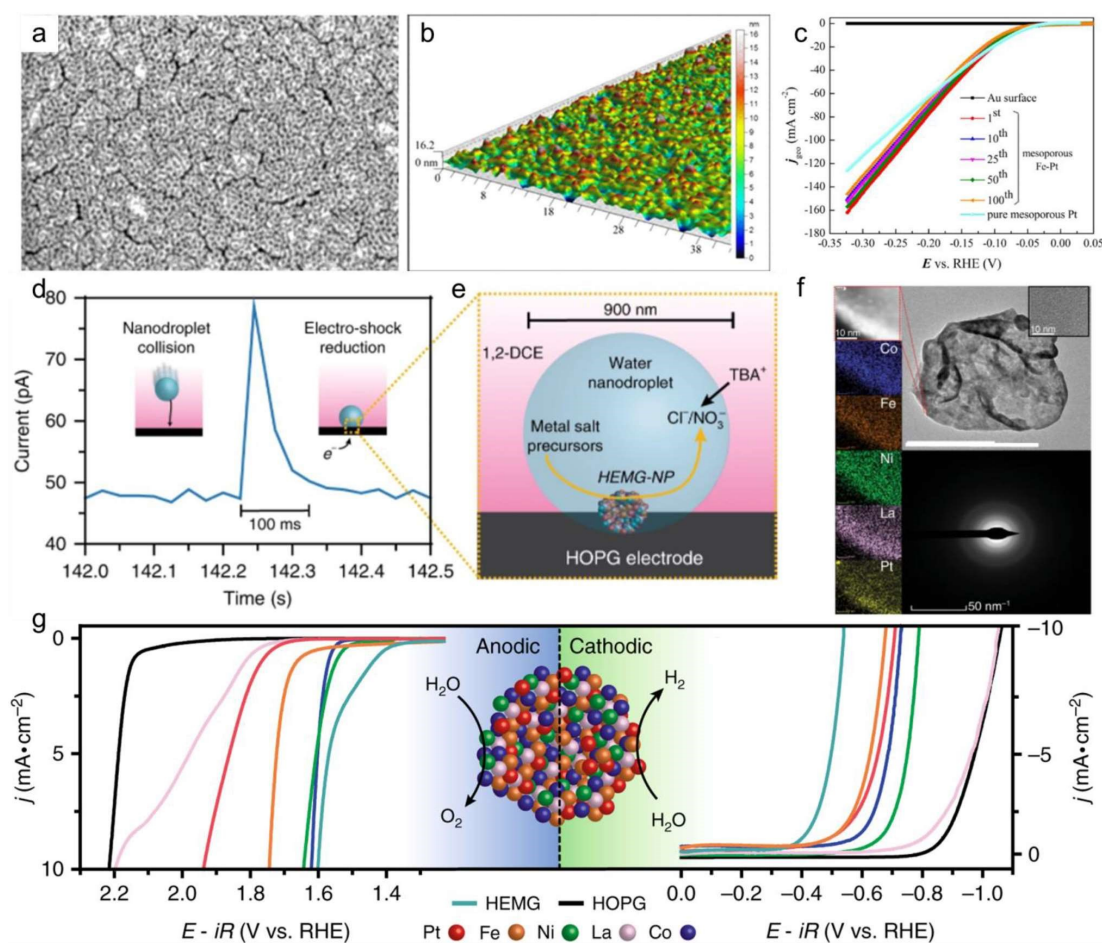


**Figure 8** a-b) SEM (a) and confocal (b) images of mesoporous Fe-Pt film electrodeposited on Au. c) LSV curves of the Fe-Pt film on Au. Reproduced with permission from Ref. 73. Copyright 2018 John Wiley and Sons. d-e) Current response to the nanodroplet collision onto a carbon fiber ultramicroelectrode (d), with the scheme (e) of rapid NP formation at the interface. f) HAADF-STEM images of a CoFeNiLaPt NP with high-resolution EDS images and SAED pattern indicating an amorphous microstructure. g) Electrocatalytic water electrolysis test of CoFeNiLaPt NP (turquoise curve) and each of its components. Reproduced with permission from Ref. 79. Copyright 2019 Springer Nature. (color on line)

For example, Zhang's group constructed ultrathin NiFe layered double hydroxide nanosheets with W-doping via a facile electrodeposition process (Figure 9) [87]. By putting carbon paper (CP) into an aqueous electrolyte containing the metal ions, nanosheets can *in situ* grow on its surface at  $-1.0$  V vs. Ag/AgCl. Adding W<sup>6+</sup> into the electrolyte leads to W doping, which enhances the electrical conductivity. As a result, the NiFeW/CP exhibits only 239 and 115 mV overpotentials at  $10 \text{ mA} \cdot \text{cm}^{-2}$  for OER and HER, respectively, as a bifunctional catalyst in  $1 \text{ mol} \cdot \text{L}^{-1}$  KOH. Ma et al. fabricated ultrathin nanosheet arrays of Co<sub>3</sub>O<sub>4</sub> and Co(OH)<sub>2</sub> via a two-step electrochemical

synthesis protocol: electrodeposition of Co<sub>0.85</sub>Se and then anodic oxidation/cathodic reduction, which effectively catalyze the overall water electrolysis in alkaline and neutral electrolyzers [88].

In addition to TMOs, TMPs have gained increasing attentions as promising HER catalyzing candidates in recent years for their high proton-trapping ability of highly electronegative P atoms [89], which are very capable of electrochemical synthesis [90-93]. For example, Sun et al. developed a facile potentiodynamic electrodeposition method using common cobalt sulfate and sodium hypophosphite monohydrate [94]. By applying consecutive linear scan between  $-0.3$  and  $-1.0$  V vs.

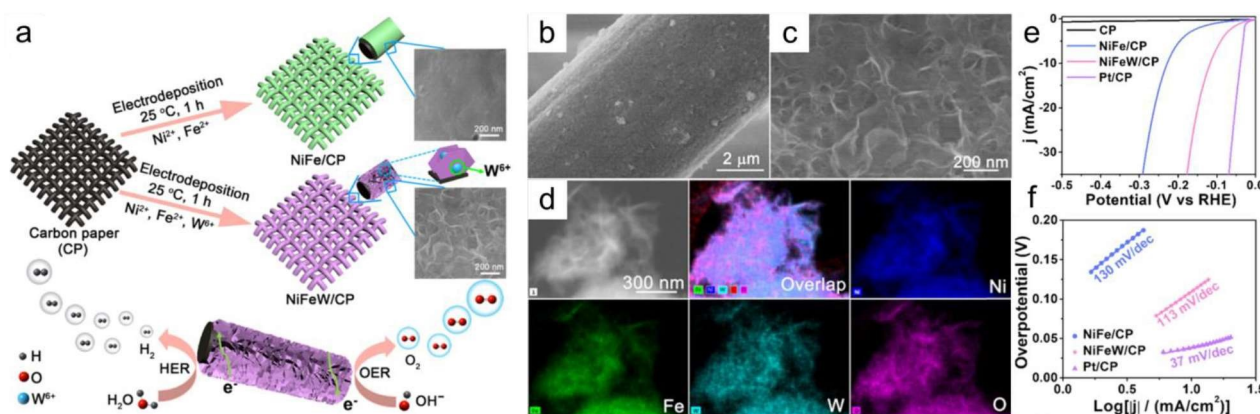


**Figure 9** a) Scheme for the one-step electrochemical synthesis of the NiFeW/CP. b-d) SEM (b, c) and STEM-EDS (d) images of the morphology and elemental distribution of the NiFeW/CP. e-f) HER polarization (e) and Tafel (f) curves of the NiFeW/CP and control groups. Reproduced with permission from Ref. 87. Copyright 2021 American Chemical Society. (color on line)

Ag/AgCl, they evenly deposited amorphous Co-P film on a copper foil under rotation, stirring conditions and  $N_2$  atmosphere. The as-prepared catalyst exhibits good performance of  $-94$  and  $345$  mV overpotentials,  $42$  and  $47$   $mV \cdot dec^{-1}$  Tafel slopes at  $10$   $mA \cdot cm^{-2}$  for HER and OER, respectively. With this bifunctional catalyst, the overall water splitting can be performed over  $1.56$  V with a  $69$   $mV \cdot dec^{-1}$  Tafel slope and  $100\%$  FE, rivaling the mature  $IrO_2/Pt-C$  system. Using this technique, they further deposited uniform Co-P on copper foam, which shows good bifunctional catalyzing performance towards both HER and 5-hydroxymethylfurfural oxidation, discussed in a later section<sup>[95]</sup>.

To date, TMD is one of the largest groups of materials engaged in electrochemistry. Various materials like  $MoS_2$ <sup>[96-100]</sup>,  $WS_2$ <sup>[101, 102]</sup>, 3rd-row TMDs<sup>[103]</sup>, etc. with fascinating structures and electronic states have been electrochemically synthesized and modified to catalyze HER better. For example, Shaijumon's group synthesized luminescent  $MoS_2$  quantum dots via an electrochemical etching method<sup>[97]</sup>. They put bulk  $MoS_2$  in aqueous solutions of 1-butyl-3-methylimidazolium chloride ionic liquid and lithium bis-tri fluoromethylsulfonylimide to electrochemically etch it towards quantum dots. A good size control over the quantum dots can be achieved by tuning the applied potential and electrolyte composition. The  $MoS_2$

quantum dots demonstrate a small Tafel slope and high exchange-current density for HER in  $0.5$   $mol \cdot L^{-1}$   $H_2SO_4$ , which is due to a large number of active edge sites in quantum dots. The crystal structures (hexagonal, trigonal, rhomboedric) and therefore the electronic configuration of  $MoS_2$  can also be adjusted via electrochemical synthesis approaches<sup>[104]</sup>. Cui et al. built nanostructured  $MoS_2$  into a battery-like system and utilized its interlayer expansion during lithium intercalation to exfoliate it from semiconducting 2H phase to metallic 1T phase (Figure 10)<sup>[105]</sup>. The resulted catalyst demonstrated  $200$   $mA \cdot cm^{-2}$  HER current density at only  $200$  mV overpotential.

TMCs have received huge attention as HER catalysts in recent years for their high-cost efficiency, electrical conductivity, chemical and thermal stabilities, and similar electrochemical peculiarity to Pt-based catalysts<sup>[106, 107]</sup>. In 2018, Wang's group electrochemically synthesized N-doped  $Mo_2C$  nanoparticles through a one-step solid-state electrolytic reduction<sup>[108]</sup>. The mixtures of  $MoS_2$  and carbon precursors are electrolytically reduced in molten  $CaCl_2$  at  $850$   $^{\circ}C$ , leading to a series of  $Mo_2C$  materials. Using PPy as the carbon precursor leads to N-doped  $Mo_2C$  with near-spherical nanoparticle morphology. The N doping facilitates active center exposure and modifies the nanoparticle electronic property, therefore leading to a low onset potential of  $78.1$  mV and a Tafel slope of

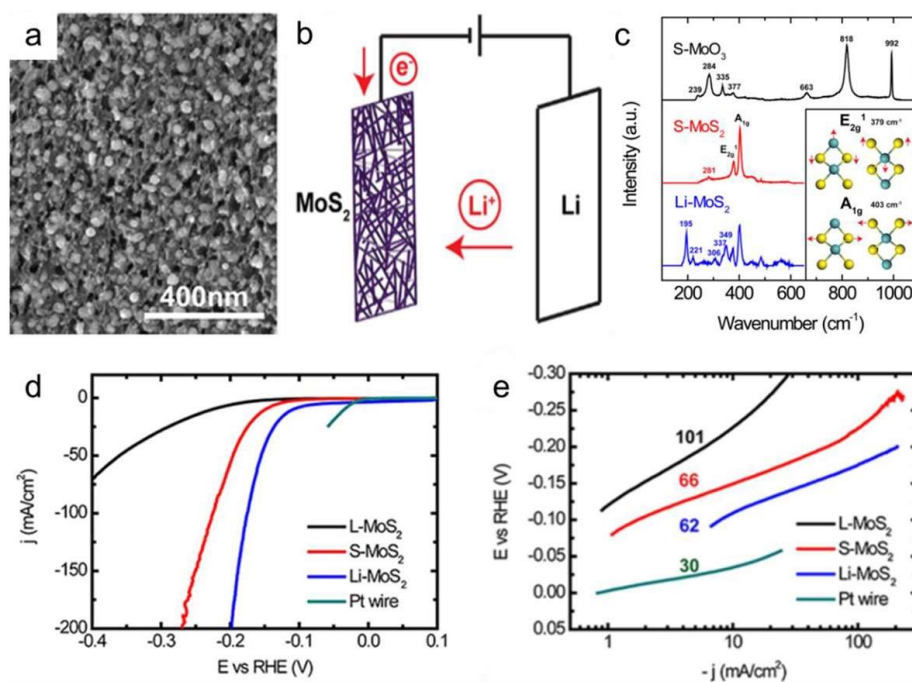


**Figure 10** a) SEM image of the as-grown MoS<sub>2</sub> NPs on carbon film. b) Scheme of the lithium intercalation setup to tailor the structure of MoS<sub>2</sub>. c) Raman spectra of MoS<sub>2</sub> samples indicating 1T phase formation after lithiation. d) Polarization curves of MoS<sub>2</sub> samples catalyzing HER. e) Tafel plots of L-MoS<sub>2</sub>, S-MoS<sub>2</sub>, Li-MoS<sub>2</sub>, and Pt wire. Reproduced with permission from Ref. 105. Copyright 2014 American Chemical Society. (color on line)

59.6 mV · dec<sup>-1</sup> for HER in 0.5 mol · L<sup>-1</sup> H<sub>2</sub>SO<sub>4</sub>, as well as high activity and stability in a broad pH range (0 ~ 14). Furthermore, the synthesis method can be extended to other TMCs like NbC, TiC, and WC<sup>[109]</sup>.

In addition to the abovementioned transition metal compounds, some other catalysts like metal-organic frameworks (MOFs)<sup>[110, 111]</sup> and hydroxyphosphates<sup>[112]</sup> have also been electrochemically attempted. For example, Gong's group synthesized terephthalate (tp)-based MOFs of transition metals through a one-step electrodeposition<sup>[113]</sup>. Being used as HER catalyst, the Ni<sub>3</sub>(OH)<sub>2</sub>(H<sub>2</sub>O)<sub>2</sub>(tp)<sub>2</sub> shows only 60 mV overpotential at 10 mA · cm<sup>-2</sup>, which is comparable to commercial Pt/C catalyst. With the help of scanning electrochemical microscopy (SECM), Hod et al. achieved localized electrosyntheses of Al<sub>2</sub>(OH)<sub>2</sub>-TCPP and HKUST-1 MOFs<sup>[114]</sup>. The general SECM-assisted electrochemical synthesis setup involves SECM tip as the working electrode and Pt wire as the counter and reference electrodes. During synthesis, the SECM tip was cycled between -0.55 to -1.75 V versus Pt to reduce

H<sub>2</sub>O into OH<sup>-</sup>, which deprotonates the H<sub>4</sub>TCPP ligands and reacts with Al<sub>2</sub>O<sub>3</sub> to release Al<sup>3+</sup>. The Al<sub>2</sub>(OH)<sub>2</sub>-TCPP MOF then forms locally at the substrate-tip gap due to the high local concentration. SECM was also used to evaluate the electrocatalytic activity of the MOFs by scanning over the surface ~10 μm above the catalyst and recording the tip current corresponding to H<sub>2</sub> generation kinetics.

Electrochemical composition of multiple catalysts is a promising approach towards more efficient hydrogen production<sup>[115-119]</sup>. For example, Sun, et al. developed a two-step electrodeposition-electropolymerization strategy to fabricate polyaniline-coated nickel on nickel foam (PANI/Ni/NF) (Figure 11a)<sup>[119]</sup>. They firstly electrodeposited Ni nanoparticles onto NF, which shows porous microsphere morphology benefited from simultaneously generated H<sub>2</sub> bubbles. Then, they used the Ni/NF as the working electrode to perform electropolymerization of aniline at a 0.5 mA · cm<sup>-2</sup> current density for 1000 s, leading to a uniform PANI coating layer (Figure 11b). The resulted



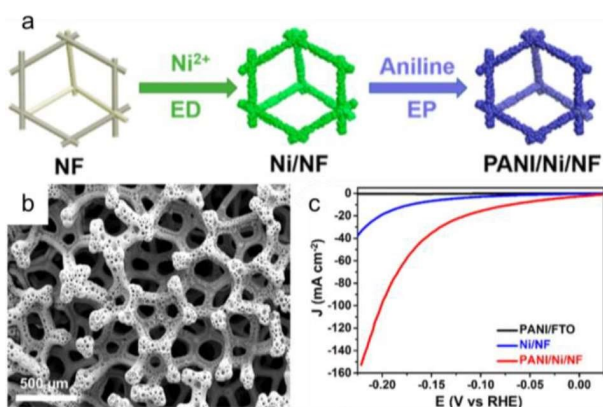


**Figure 11** a) Scheme of the two-step electrodeposition-electropolymerization preparation of PANI/Ni/NF. b) SEM image of PANI/Ni/NF. c) LSV plots of PANI/Ni/NF with control groups in  $1.0 \text{ mol} \cdot \text{L}^{-1}$  KOH. Reproduced with permission from Ref. 119. Copyright 2018 American Chemical Society. (color on line)

PANI/Ni/NF demonstrated superior HER catalyzing activity of 72 mV overpotentials at  $10 \text{ mA} \cdot \text{cm}^{-2}$  than bare Ni or PANI (Figure 11c). Such electropolymerization strategy can also be extended to nickel phosphides and sulfides. Wiley's group fabricated Cu-Pt core-shell nanowires by electroplating Pt onto Cu<sup>[120]</sup>. The electroplating minimizes galvanic replacement and retains the electronic conductance of Cu, therefore eliminating the need for conductive substrates. As such, the Cu-Pt nanowires exhibit mass activities up to 8 times higher than the commercial Pt/C electrode, while the films are robust and flexible. In consid-

ering the sluggish kinetics of alkaline HER, Markovic et al. composited clusterly  $\text{Ni}(\text{OH})_2$  onto Pt electrode by electrodeposition<sup>[121]</sup>. The resulted Pt- $\text{Ni}(\text{OH})_2$  composite demonstrated an 8-fold enhancement in the activity, revealing the dual-site reaction mechanism: an oxide holds water dissociation and a metal facilitates  $\text{H}^+$  adsorption, association, and  $\text{H}_2$  desorption.

Apart from fabricating materials, electrochemical approaches are also efficient in tuning the properties of existing electrocatalysts<sup>[38]</sup>. This includes but not limited to the tuning of electronic structure<sup>[122, 123]</sup>, crystallinity and phase<sup>[124, 125]</sup>, lattice strain<sup>[126]</sup>, etc. For example, Yang's group electrochemically modified the electronic structure of  $\text{IrO}_2$  nanoparticles by partially reducing Ir(+4) and trace depositing Pt using a CV process<sup>[122]</sup>. This lowers the hydrogen adsorption energy of  $\text{IrO}_2$  and thus promotes its HER kinetics. As a result, the as-prepared Pt- $\text{IrO}_2$ /carbon with  $36.6 \mu\text{g} \cdot \text{cm}^{-2} (\text{Ir+Pt})$  shows excellent HER activities of 5, 22, and 26 mV overpotentials at  $10 \text{ mA} \cdot \text{cm}^{-2}$  in  $0.5 \text{ mol} \cdot \text{L}^{-1} \text{H}_2\text{SO}_4$ ,  $1.0 \text{ mol} \cdot \text{L}^{-1} \text{KOH}$ , and  $1.0 \text{ mol} \cdot \text{L}^{-1}$  phosphate buffer solution, respectively. Without exfoliating them, Cui, et al. continuously electrochemically tuned the electronic structure of vertically aligned  $\text{MoS}_2$  nanofilms by intercalation of Li into the interlayer<sup>[124]</sup>. As a result, the interlayer distance, Mo oxidation state, the 2H-to-1T phase ratio, and therefore the HER catalytic activity can be continuously tuned. They also utilized the interlayer distance changes during lithiation/delithiation of lithium-ion

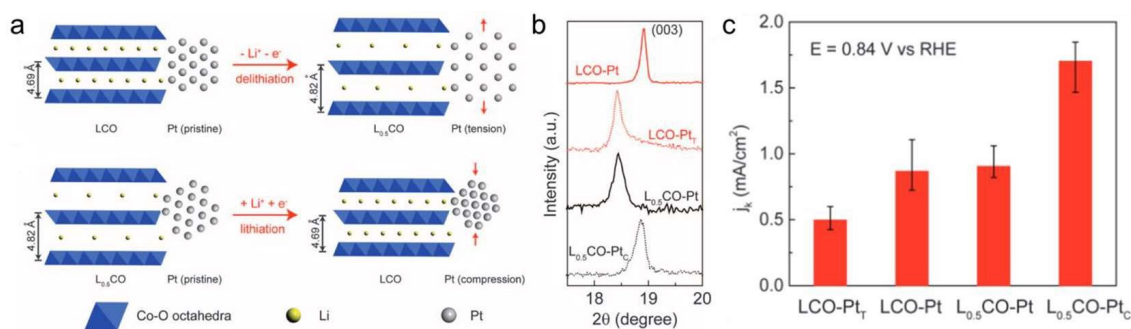


**Figure 12** a-b) Schematic illustration of interlayer space changes during lithiation/delithiation of LCO and therefore the *in situ* strain applicable on Pt clusters. b) The XRD patterns of LCO (003) peak indicating the strain. c) The comparison of oxygen reduction activities of strained Pt clusters. Reproduced with permission from Ref. 126. Copyright 2016 American Association for the Advancement of Science. (color on line)



battery electrode to control the strain and therefore the performance of Pt nanoclusters deposited on it (Figure 12)<sup>[126]</sup>. They deposited Pt nanoclusters onto pre-lithiated lithium cobalt oxide (LCO) electrodes, then continuously controlled their lattice strain by electrochemically switching the charging and discharging states. As a result, lattice compression and tension of  $\sim 5\%$  can be achieved for individual Pt nanoclusters, which leads to 90% enhancement and 40% suppression of the catalytic performance, respectively.

## 4 Electrochemical Oxidations of Small Molecules towards Cocatalysis with Hydrogen Evolution

### 4.1 Sacrificial Agent Oxidations

A straightforward way to beat the sluggish OER for more practical water electrolysis hydrogen generation is to replace it using faster oxidations with smaller onset potentials and less contaminating products. Various organics molecules such as hydrazine and urea have been attempted as the sacrificial agent for less energy-intensive hydrogen evolution<sup>[18]</sup>. For example, hydrazine is a good candidate of sacrificial agents for HER. It is industrially significant, water-miscible, and has lower oxidation potential ( $-0.33$  V vs. normal hydrogen electrode (NHE), same for the following reactions, unless specified) with no catalytic- or environmental-poisoning products<sup>[127-129]</sup>. The HzOR simply cracks hydrazine into nitrogen and water with the aid of hydroxide groups. Using a bifunctional  $\text{Ni}_2\text{P}$  catalyst, the two-electrode electrolyzer with  $1.0 \text{ mol} \cdot \text{L}^{-1}$  KOH and  $0.5 \text{ mol} \cdot \text{L}^{-1}$  hydrazine achieves  $500 \text{ mA} \cdot \text{cm}^{-2}$  high current density at only  $1.0$  V, with high stability and nearly 100% Faradic efficiency (FE) for HER, far suppressing the counterpart without hydrazine (Figure 13a-c)<sup>[128]</sup>. Various bifunctional catalysts like  $\text{CoSe}_2$  and  $\text{RuP}_2$  have been developed with advanced HzOR-HER performances<sup>[130-134]</sup>. Apart from alkaline electrolyzers, hydrazine also serves the sacrificial role well in seawater electrolysis, a more cost-effective and grid-scale approach to hydrogen production, by beating the chlorine evolution with its

lower potential<sup>[135-138]</sup>. On NiCo/MXene-based electrodes, it reports a  $9.2 \text{ mol} \cdot \text{h}^{-1} \cdot \text{gcat}^{-1}$  hydrogen generation rate with a low electricity cost of  $2.75 \text{ kWh} \cdot \text{m}^{-3}$  of  $\text{H}_2$  at  $500 \text{ mA} \cdot \text{cm}^{-2}$ , which is 48% lower than the commercial alkaline water electrolysis (Figure 13d-f)<sup>[135]</sup>. The device can be further made into self-powered by integrating with direct hydrazine fuel cells or solar cells<sup>[135, 139, 140]</sup>.

After the pioneering sacrificial HER attempt<sup>[127]</sup>, various other sacrificial agents like urea<sup>[141-146]</sup>, ammonia<sup>[147]</sup>, and sodium borohydride with high water solubility and lower oxidation potentials have also been intensively attempted to replace the OER. For example, combining with UOR in the bifunctional CoMn/CoMn<sub>2</sub>O<sub>4</sub> catalyzed alkaline electrolyzer, HER shows only  $-0.069$  V to reach  $10 \text{ mA} \cdot \text{cm}^{-2}$ , with only  $1.51$  V two-electrode cell potential (Figure 14a, b)<sup>[144]</sup>. The urea is oxidized into nitrogen, carbon dioxide, and water during the process. While urea is abundant from various wastewater, UOR-mediated water electrolysis offers an efficient and adaptable route for simultaneous hydrogen evolution and wastewater treatment, both economically and ecologically (Figure 14c)<sup>[143, 148-150]</sup>. Another frequently used sacrificial reaction is AOR, which converts ammonia with hydroxide groups into nitrogen and water<sup>[75, 151-154]</sup>. It is also industrially important, environmentally friendly, and more thermodynamically favourable than OER ( $-0.77$  V). With a PtRu bimetallic bifunctional catalyst, HER shows  $37.6 \text{ mV}$  over potential at  $10 \text{ mA} \cdot \text{cm}^{-2}$ , with the AOR as the counter reaction at an overall cell potential of just  $0.72$  V in an alkaline electrolyser<sup>[155]</sup>.

### 4.2 Value-Adding Electrochemical Oxidation of Small Molecules

Although sacrificial agents efficiently promote hydrogen evolution by reducing the overall potential and powering the kinetics, they increase the cost of water electrolysis without any valuable product but just  $\text{CO}_2$  and  $\text{N}_2$ , etc. As such, a more economical and efficient approach is to introduce oxidations that are more favorable than OER, meanwhile convert sacrificial precursors into value-added products<sup>[156, 157]</sup>. This usually lies in the oxidation of various less-valuable

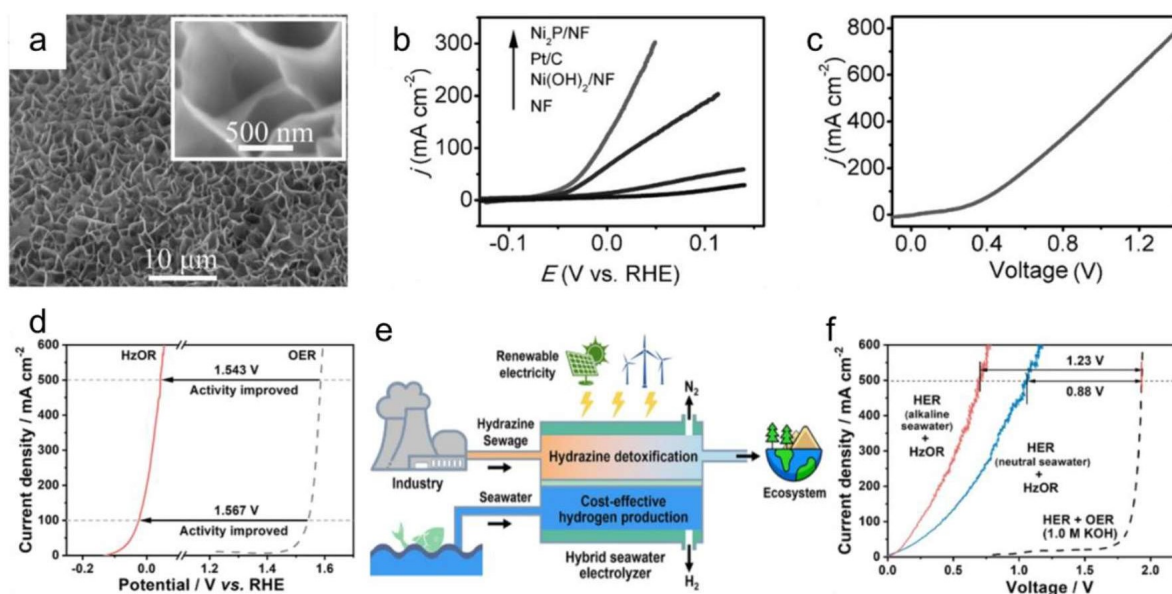


**Figure 13** a) SEM image of Ni<sub>2</sub>P nanosheet on Ni foam. b-c) LSV curves of various catalysts towards HzOR in 1 mol·L<sup>-1</sup> KOH and 0.5 mol·L<sup>-1</sup> hydrazine (b), and of Ni<sub>2</sub>P catalyzed hydrazine-assisted HER in a two-electrode configuration. Reproduced with permission from Ref. 128. Copyright 2017 John Wiley and Sons. d) LSV curves of NiCo/MXene catalyzing HzOR or OER in 1.0 mol·L<sup>-1</sup> KOH with/without 0.5 mol·L<sup>-1</sup> hydrazine, highlighting the favoured HzOR over OER. e) Scheme of a cost-effective and sustainable hydrogen production by renewable-powered seawater electrolyzer with sea water and industrial hydrazine sewage as feeds. f) LSV curves of hydrazine-assisted water electrolysis hydrogen productions compared to alkaline water electrolysis. Reproduced with permission from Ref. 135. Copyright 2021 Springer Nature. (color on line)

small molecules towards more industrially important intermediates and/or products. Alcohol (ethanol, benzyl alcohol, ethylene glycol, etc.) oxidations represent a big group of organics electrochemical synthesis, which adds oxygens to and/or remove hydrogens from the hydroxylated carbons towards carboxylic acids, ketones, aldehydes, etc. or even CO and CO<sub>2</sub> at lower potentials than OER<sup>[158, 159]</sup>. They have been intensively investigated in direct alcohol fuel cells and alcohol-assisted water electrolysis (electrochemical alcohol reforming) for their cost-effectiveness in converting many petroleum and biomass-derived feedstocks into value-added chemicals under mild potentials (Figure 15a)<sup>[159-161]</sup>. Taking ethanol as an example, it usually shows lower onset potentials than other alcohols and can save up to 92% energy consumption for hydrogen generation than that with alkaline water<sup>[162-164]</sup>. Using metallic or oxide catalysts, an ethanol-assisted water electrolyzer can generate hydrogen with 10 mA·cm<sup>-2</sup> and more than 98% FE at

potentials lower than 1 V, compared to more than 1.5 V of alkaline water electrolysis (Figure 15b, c)<sup>[164, 165]</sup>. Simultaneous with HER, the ethanol can be oxidized to acetates and ethyl acetate that are more valuable than O<sub>2</sub>, and therefore further improve the efficiency of water electrolysis<sup>[163, 164, 166]</sup>. Glycerol is also a frequently studied value-adding sacrificial agent, which is a low-value-added-by-product of biodiesel<sup>[167]</sup>. It can be electrochemically oxidized to lactic acid, a kind of important industrial intermediate with high value, with glyceraldehyde as the intermediate at a theoretical potential of 0.69 V, far lower than the 1.23 V of OER<sup>[168]</sup>. Catalyzed by a bifunctional Ni-Mo-N on carbon cloth, the alkaline HER-GOR electrolyzer only needs 1.36 V to achieve 10 mA·cm<sup>-2</sup>, 0.26 V lower than alkaline water electrolysis without glycerol<sup>[169]</sup>. The electrolyzer yields H<sub>2</sub> with 99.7% FE and formate with 95% FE, marking a much more efficient and profitable process than conventional water electrolysis.

While ethanol oxidizes to relatively simple prod-

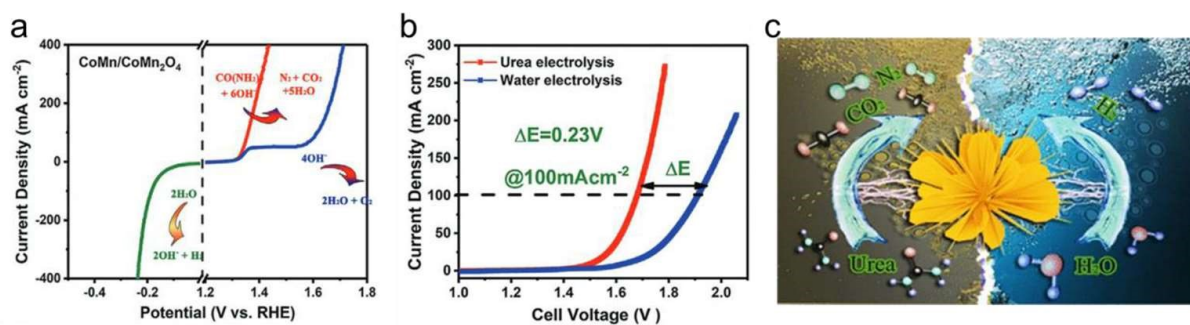


**Figure 14** a) Polarization curves of CoMn/CoMn<sub>2</sub>O<sub>4</sub> bifunctional catalyst for HER, UOR, and OER. b) Comparison in the polarization curves of CoMn/CoMn<sub>2</sub>O<sub>4</sub> catalyzing alkaline or urea water electrolysis. Reproduced with permission from Ref. 144. Copyright 2020 John Wiley and Sons. c) Scheme of urea-assisted water electrolysis to cost-effectively degrade wastewater and produce H<sub>2</sub>. Reproduced with permission from Ref. 149. Copyright 2020 American Chemical Society. (color on line)

ucts, oxidation of other alcohols often leads to complicated products like carboxylic acids, carbonates, ketones, and their mixtures. This is due to the multi-step nature of AOR, which leads to thermodynamically uphill intermediates with high kinetic barriers and retards the complete oxidation of alcohols. Finetuning the electrocatalyst allows selective oxidation towards desired products<sup>[170, 171]</sup>. For example, catalyzed by a PdAg alloy on Ni foam with tailored adsorption energy and d-band centre, a 92% high FE is achieved for selective ethylene glycol oxidation (EGOR) to glycolic acid at 10 mA · cm<sup>-2</sup> with only 0.57 V potential<sup>[171]</sup>.

Recently, electrochemical synthesis-assisted HER has attracted much attention and many other value-adding biomass-derived compounds like carbohydrates<sup>[172-174]</sup>, amines<sup>[175-178]</sup>, and aldehydes<sup>[95, 179, 180]</sup> have been attempted. For example, glucose is one of the most abundant biomass-based chemicals and an important industrial precursor for commodity chemicals like sorbitol and glucaric acid (GRA)<sup>[181]</sup>. Electrochemical oxidation can convert glucose into abundant products like fructose, 5-hydroxymethyl furfural (HMF), carboxylic acids, etc. by direct oxidation, isomerization, dehydration, etc<sup>[182]</sup>. Compared to traditional chemical oxidation or microbial fermentation, it eliminates the requirements of high-pressure O<sub>2</sub> and hazardous oxidants, can be performed under milder conditions, and produces fewer by-products via tuning reaction parameters. It is suitable especially at a small scale and the cost efficiency can be even

higher with the lower price of renewable electricity<sup>[183]</sup>. With lower oxidation potential (0.05 V) than OER, glucose oxidation can efficiently couple with HER to generate H<sub>2</sub> at the cathode and GRA at the anode simultaneously towards higher economic efficiency, from both hydrogen and GRA production points of view<sup>[172, 184, 185]</sup>. In 2020, Yu's group designed nanostructured NiFe oxides and nitrides as bifunctional catalysts for glucose-assisted water electrolysis, with which the glucose oxidation demonstrates superior 1.13 V onset potential and 19 mV · dec<sup>-1</sup> Tafel slope, leading to an 87% higher FE and 83% yield for GRA production (Figure 16)<sup>[172]</sup>. The two-electrode electrolyzer with NiFeO<sub>x</sub> as the anode and NiFeN<sub>x</sub> as the cathode delivers 200 mA · cm<sup>-2</sup> high current density at only 1.48 V, leading to a 54% cost reduction compared to current chemical approach.

Another typical example is the oxidation of HMF<sup>[95]</sup>. It is the dehydration product of reducing sugars and is used in the food industry. It can be electrochemically converted to 2,5-furandicarboxylic acid (FDCA), which is an important monomer for polymeric fabrications, by oxidizing the terminal hydroxylated carbon and aldehyde group into carboxy groups at a lower potential than OER. Therefore, it can couple with hydrogen evolution<sup>[186, 187]</sup>. For example, Sun's lab developed a 3D Ni<sub>2</sub>P nanoparticle arrays on nickel foam (Ni<sub>2</sub>P NPA/NF) bifunctional electrocatalyst to couple HMF oxidation with HER in an alkaline electrolyzer (Figure 17a-e)<sup>[179]</sup>. The system achieved a

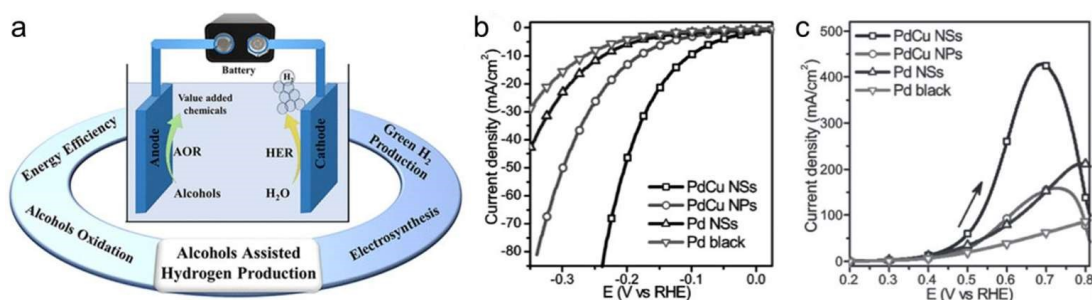


**Figure 15** a) Scheme of the electrocatalytic, alcohol-assisted hydrogen productions that save energy and generate value-adding products. Reproduced with permission from Ref. 159. Copyright 2021 American Chemical Society. b-c) LSV polarization curves for the HER (b) and ethanol oxidation (c) catalysing with bifunctional 3D PdCu NSs, PdCu NPs, Pd NSs, and Pd black. Reproduced with permission from Ref. 165. Copyright 2017 John Wiley and Sons. (color on line)

high current density of  $50 \text{ mA} \cdot \text{cm}^{-2}$  with a voltage 200 mV smaller than the counterpart without HMF added. The FE values for both HER (100%) and HMF oxidation (98%) are high, together with the high catalysing stability, indicating the superiority of this system. They also used an electrodeposited Co-P electrocatalyst to achieve a  $20 \text{ mA} \cdot \text{cm}^{-2}$  current density at 1.38 V for HMF oxidation with 90% FDCA yield in a  $1.0 \text{ mol} \cdot \text{L}^{-1}$  KOH electrolyzer with  $50 \text{ mmol} \cdot \text{L}^{-1}$  HMF<sup>[94]</sup>. The two-electrode system with bifunctional Co-P achieved  $20 \text{ mA} \cdot \text{cm}^{-2}$  at 1.44 V with nearly 100% FE, superior to that with OER. In addition, other furan compounds like furfuryl, furfural alcohol

have also been demonstrated by Sun, et al. to have favorable oxidation than water, with lower onset potentials and non-polluting, value-adding products (Figure 17f, g)<sup>[180]</sup>.

In addition to organic electrochemical synthesis,  $\text{H}_2\text{O}_2$  is an extremely valuable inorganic commodity chemical. Nowadays, it is mainly produced based on the catalytic reduction of oxygen, named the anthraquinone process, which is not sustainable with scarce catalysts and high energy consumption<sup>[23]</sup>. Alternatively, the electrochemical synthesis of  $\text{H}_2\text{O}_2$  is a more eco-friendly route via oxygen reduction (0.68 V) or water oxidation (1.77 V)<sup>[188]</sup>. The latter could be

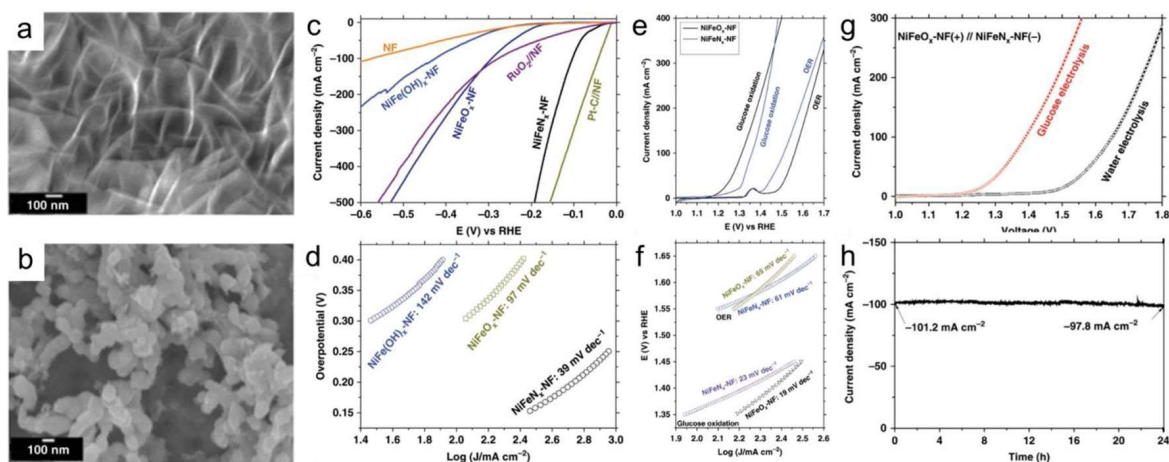


**Figure 16** a-b) SEM images of the  $\text{NiFeO}_x$ -Ni foam (a) and  $\text{NiFeN}_x$ -Ni foam (b). c-f) The LSV (c, e) and Tafel slopes (d, f) of  $\text{NiFeO}_x$  and  $\text{NiFeN}_x$  for HER (c, d) and GEOR (e, f) in  $1 \text{ mol} \cdot \text{L}^{-1}$  KOH with glucose concentration of  $100 \text{ mmol} \cdot \text{L}^{-1}$  under  $5 \text{ mV} \cdot \text{s}^{-1}$  scan rate. g-h) Polarization comparison between glucose or alkaline water electrolysis (g) and long-term stability of glucose electrolysis at 1.4 V cell potential. Reproduced with permission from Ref. 172. Copyright 2020 Springer Nature. (color on line)



highly effective by reforming the only precursor, water, into  $H_2$  and  $H_2O_2$  simultaneously within one electrolyzer, after competing with the lower potential OER<sup>[189-191]</sup>. For example, MacFarlane et al. demonstrated water electrochemical oxidation over a  $MnO_x$  catalyst, producing both  $H_2$  and  $H_2O_2$  without  $O_2$  evolution<sup>[192]</sup>. The reaction took place in a butyl ammonium bisulfate electrolyte, which works together with the catalyst leading to only 150 mV overpotential at  $1\text{ mA}\cdot\text{cm}^{-2}$ , and helps to stabilize the  $H_2O_2$  by solvation. Facilitated by solar energy, Sayama et al. were able to further reduce the reaction potential even lower than the theoretical one<sup>[190]</sup>. They designed a photo-electrode system with a  $WO_3/BiVO_4$  photoanode, which achieves 54% selectivity and  $2\text{ mmol}\cdot\text{L}^{-1}$  accumulation for  $H_2O_2$  at  $5^\circ\text{C}$  in  $2.0\text{ mol}\cdot\text{L}^{-1}\text{ KHCO}_3$  electrolyte.

## 5 Future Perspectives

Despite numerous achievements that have been down, there remain many challenges and opportunities along the journey of electrochemical synthesis-assisted water splitting towards practical applications.

Firstly, although many electrodeposition and elec-

trochemical exfoliation strategies have been developed to fabricate effective water electrolysis catalysts, they are usually unfeasible for advanced nanostructures and compositions. This is especially true for transition metal compounds, which usually adopt complicated compositions and crystal structures, nanostructures beyond the scope of conventional electrochemical synthesis. Considering the inherent limitations of those methods, developing novel and interdisciplinary electrochemical synthesis systems with new reaction designs and/or introducing characters from other electrochemical systems (batteries<sup>[126]</sup>, capacitors<sup>[193]</sup>, etc.) into synthesis processes, is desired to open new avenues for electrochemical synthesis in water electrolysis and other fields.

Secondly, although co-electrolytic hydrogen production has been proven an efficient alternative to intrinsic water electrolysis, and many sacrificial or value-adding routes have been developed, discovering and developing new co-electrolysis systems with lower energy consumption, faster kinetics, and more valuable processes is always desired. There remain many attractive electrochemical oxidation processes like  $CO_2$  oxidation<sup>[194]</sup>, and nitrogen oxidation<sup>[195, 196]</sup>, with

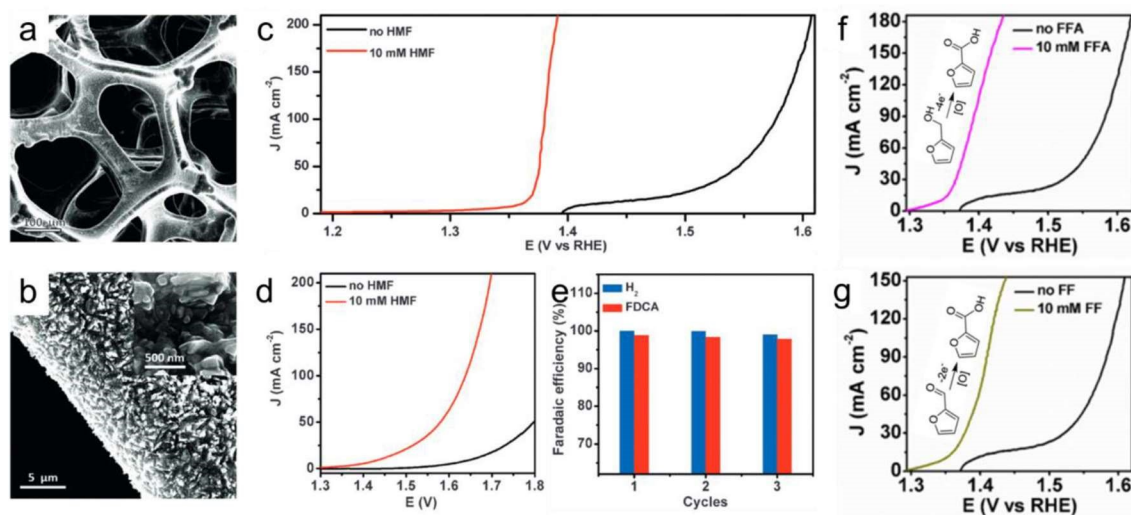


**Figure 17** a-b) SEM images of the  $Ni_2P$ -based catalyst. c-d) LSV curves of  $Ni_2P$ -based catalyst in  $1\text{ mol}\cdot\text{L}^{-1}\text{ KOH}$  with/without  $10\text{ mmol}\cdot\text{L}^{-1}\text{ HMF}$  under  $2\text{ mV}\cdot\text{s}^{-1}$  scan rate for HMF oxidation (c) and HMF-assisted water electrolysis (d). e) The FE for both hydrogen and FDCA generation as shown in (c, d). Reproduced with permission from Ref. 179. Copyright 2016 John Wiley and Sons. f-g) LSV curves of the oxidations of furfuryl alcohol (FFA) (f) and furfuryl (FF) using a  $Ni_3S_2$ -based catalyst. Insets show the chemical formula. Reproduced with permission from Ref. 180. Copyright 2016 American Chemical Society. (color on line)

favoured lower potentials and/or value-adding products that are promising for co-electrolysis with HER but hindered by some inherent limitations. Integrating these reactions with HER will bring co-electrolytic hydrogen production to a new height. Moreover, efficient separation and purification of the co-electrolysis products are also key factors for their practical applications.

Thirdly, although intensive mechanism investigations have been done on the original water electrolysis consisted of HER and OER, working principles of co-electrolysis systems are different from those and remain poorly attained. In co-electrolysis systems, more than one kind of analytes are added, and more than one kind of products are obtained. The catalyzing mechanisms of anodic oxidations, the interactions of chemical species, and their influences on HER should be brought to the forefront to better understand and therefore develop co-electrolysis systems towards more efficient hydrogen and value-adding species production. *In situ* and operando characterization such as X-ray spectroscopy and TEM, as well as theoretical analysis such as DFT and MD can be pivotal in revealing the scientific basis<sup>[193, 197]</sup>. Moreover, the oxidations of biomasses and nucleophiles could be enlightening in this field.

Fourthly, in addition to exploring and optimizing co-electrolysis reactions, designing advanced catalysts for the systems is of equal importance. Considering the wide variety of co-electrolysis systems, no general catalyst may be available and specific catalysts should be designed for specific systems. Currently, most of the co-electrolysis systems are driven by bifunctional catalysts, which catalyze both HER and oxidations within one uniform system. With a deeper understanding of various electrochemical oxidations, specific catalysts for the anode, or bifunctional catalysts that are specifically efficient for the designated system with high activity, selectivity, and durability should be developed, accompanied by the mechanism investigations.

## 6 Conclusions

This review summarizes the current status of

electrochemical syntheses applied in the field of water electrolysis hydrogen production, both in terms of fabricating novel electrocatalysts and developing OER- alternating co-electrolysis systems. In the paper, the concepts of electrochemical synthesis and various protocols, methods for building appropriate synthetic systems are firstly introduced. For fabricating nanostructured HER catalysts, electrodeposition, electrochemical exfoliation, as well as electrochemical modification have been utilized to synthesize metallic catalysts including noble metals, alloys, transition metals, and metal compound catalysts including TMOs, TMPs, TMDs, TMCs, MOFs, etc. The effects of tuning the synthetic potential, current, time, solvent, supporting electrolyte, additive, and substrate, etc. have been discussed. In terms of replacing OER for co-electrolytic HER, both sacrificial oxidations like HzOR, UOR, AmOR, and value-adding electrosynthesis like AOR, CHOR, AhOR, WOR, etc. have been summarized. Lastly, we discussed current challenges and opportunities for electrochemical synthesis towards practical electrolytic hydrogen production as well as other electrochemical applications, which provides guidelines for future research.

## Acknowledgements:

The authors acknowledge financial supports from Singapore Ministry of Education Academic Research Fund Tier 2 (Grant No. MOE-T2EP10220-0005) and Academic Research Fund Tier 1 (Grant No. RG104/18). The authors are grateful to Dr. Zhisheng Lü and Mr. Haoyang Fu for helpful discussion.

## References:

- [1] Zhu J, Hu L S, Zhao P X, Lee L Y S, Wong K Y. Recent advances in electrocatalytic hydrogen evolution using nanoparticles[J]. *Chem. Rev.*, 2020, 120(2): 851-918.
- [2] Vesborg P C K, Seger B, Chorkendorff I B. Recent development in hydrogen evolution reaction catalysts and their practical implementation[J]. *J. Phys. Chem. Lett.*, 2015, 6 (6): 951-957.
- [3] Seh Z W, Kibsgaard J, Dickens C F, Chorkendorff I B, Nørskov J K, Jaramillo T F. Combining theory and experiment in electrocatalysis: Insights into materials design[J].

- Science, 2017, 355(6321): eaad4998.
- [4] Zou X X, Zhang Y. Noble metal-free hydrogen evolution catalysts for water splitting[J]. *Chem. Soc. Rev.*, 2015, 44 (15): 5148-5180.
  - [5] Dubouis N, Grimaud A. The hydrogen evolution reaction: From material to interfacial descriptors[J]. *Chem. Sci.*, 2019, 10(40): 9165-9181.
  - [6] Zheng Y, Jiao Y, Jaroniec M, Qiao S Z. Advancing the electrochemistry of the hydrogen-evolution reaction through combining experiment and theory[J]. *Angew. Chem. Int. Ed.*, 2015, 54(1): 52-65.
  - [7] Li Y, Luo Z Y, Ge J J, Liu C P, X W. Research progress in hydrogen evolution low noble/non-precious metal catalysts of water electrolysis[J]. *J. Electrochem.*, 2018, 24(6): 572-588.
  - [8] Leech M C, Lam K. A practical guide to electrosynthesis [J]. *Nat. Rev. Chem.*, 2022, 6(4): 275-286.
  - [9] Li G R, Xu H, Lu X F, Feng J X, Tong Y X, Su C Y. Electrochemical synthesis of nanostructured materials for electrochemical energy conversion and storage[J]. *Nanoscale*, 2013, 5(10): 4056-4069.
  - [10] Liu R, Duay J, Lee S B. Electrochemical formation mechanism for the controlled synthesis of heterogeneous  $\text{MnO}_2/\text{poly}(3,4\text{-ethylenedioxythiophene})$  nanowires [J]. *ACS Nano*, 2011, 5(7): 5608-5619.
  - [11] Petrii O A. Electrosynthesis of nanostructures and nanomaterials[J]. *Russ. Chem. Rev.*, 2015, 84(2): 159-193.
  - [12] Therese G H A, Kamath P V. Electrochemical synthesis of metal oxides and hydroxides[J]. *Chem. Mater.*, 2000, 12(5): 1195-1204.
  - [13] Xu Y, Zhang B. Recent advances in electrochemical hydrogen production from water assisted by alternative oxidation reactions[J]. *ChemElectroChem*, 2019, 6(13): 3214-3226.
  - [14] Liu K W, Zhang C L, Sun Y D, Zhang G H, Shen X C, Zou F, Zhang H C, Wu Z W, Wegener E C, Taubert C J, Miller J T, Peng Z M, Zhu Y. High-performance transition metal phosphide alloy catalyst for oxygen evolution reaction[J]. *ACS Nano*, 2018, 12(1): 158-167.
  - [15] Li Y, Wei X F, Chen L S, Shi J L. Electrocatalytic hydrogen production trilogy[J]. *Angew. Chem. Int. Ed.*, 2021, 60(36): 19550-19571.
  - [16] You B, Han G Q, Sun Y J. Electrocatalytic and photocatalytic hydrogen evolution integrated with organic oxidation[J]. *Chem. Commun.*, 2018, 54(47): 5943-5955.
  - [17] Yan M, Kawamata Y, Baran P S. Synthetic organic electrochemical methods since 2000: On the verge of a renaissance[J]. *Chem. Rev.*, 2017, 117(21): 13230-13319.
  - [18] Chen L S, Shi J L. Co-electrolysis toward value-added chemicals[J]. *Sci. China Mater.*, 2022, 65(1): 1-9.
  - [19] Garlyyev B, Xue S, Fichtner J, Bandarenka A S, Andronesco C. Prospects of value-added chemicals and hydrogen via electrolysis[J]. *ChemSusChem*, 2020, 13(10): 2513-2521.
  - [20] Pletcher D, Walsh F C. *Industrial electrochemistry*[M]. America: Springer Dordrecht, 1993.
  - [21] Heard D M, Lennox A J J. Electrode materials in modern organic electrochemistry[J]. *Angew. Chem. Int. Ed.*, 2020, 59(43): 18866-18884.
  - [22] Izutsu K. *Electrochemistry in nonaqueous solutions*[M]. America: John Wiley & Sons, Inc., 2002.
  - [23] Campos-Martin J M, Blanco-Brieva G, Fierro J L G. Hydrogen peroxide synthesis: An outlook beyond the anthraquinone process[J]. *Angew. Chem. Int. Ed.*, 2006, 45 (42): 6962-6984.
  - [24] Yount J, Piercey D G. Electrochemical synthesis of high-nitrogen materials and energetic materials[J]. *Chem. Rev.*, 2022, 122(9): 8809-8840.
  - [25] Jovic V D, Jovic B M, Pavlovic M G. Electrodeposition of Ni, Co and Ni-Co alloy powders[J]. *Electrochim. Acta*, 2006, 51(25): 5468-5477.
  - [26] Wang J, Polleux J, Lim J, Dunn B. Pseudocapacitive contributions to electrochemical energy storage in  $\text{TiO}_2$  (anatase) nanoparticles[J]. *J. Phys. Chem. C*, 2007, 111 (40): 14925-14931.
  - [27] Mai L Q, Minhas-Khan A, Tian X C, Hercule K M, Zhao Y L, Lin X, Xu X. Synergistic interaction between redox-active electrolyte and binder-free functionalized carbon for ultrahigh supercapacitor performance[J]. *Nat. Commun.*, 2013, 4: 2923.
  - [28] Ahn S H, Hwang S J, Yoo S J, Choi I, Kim H J, Jang J H, Nam S W, Lim T H, Lim T, Kim S K, Kim J J. Electrodeposited Ni dendrites with high activity and durability for hydrogen evolution reaction in alkaline water electrolysis[J]. *J. Mater. Chem.*, 2012, 22(30): 15153-15159.
  - [29] Gurrappa I, Binder L. Electrodeposition of nanostructured coatings and their characterization—a review[J]. *Sci. Technol. Adv. Mater.*, 2008, 9(4): 043001.
  - [30] Lahiri A, Endres F. Review—electrodeposition of nanostructured materials from aqueous, organic and ionic liquid electrolytes for Li-ion and Na-ion batteries: A comparative review[J]. *J. Electrochem. Soc.*, 2017, 164(9): D597-D612.
  - [31] Walsh F C, de Leon C P. A review of the electrodeposition of metal matrix composite coatings by inclusion of particles in a metal layer: an established and diversifying



- technology[J]. *Trans. Inst. Met.*, 2014, 92(2): 83-98.
- [32] Zheng J X, Kim M S, Tu Z Y, Choudhury S, Tang T, Archer L A. Regulating electrodeposition morphology of lithium: towards commercially relevant secondary Li metal batteries[J]. *Chem. Soc. Rev.*, 2020, 49(9): 2701-2750.
- [33] Wu W M, Zhang C S, Hou S G. Electrochemical exfoliation of graphene and graphene-analogous 2D nanosheets [J]. *J. Mater. Sci.*, 2017, 52(18): 10649-10660.
- [34] Ambrosi A, Pumera M. Exfoliation of layered materials using electrochemistry[J]. *Chem. Soc. Rev.*, 2018, 47(19): 7213-7224.
- [35] Yang Y C, Hou H S, Zou G Q, Shi W, Shuai H L, Li J Y, Ji X B. Electrochemical exfoliation of graphene-like two-dimensional nanomaterials[J]. *Nanoscale*, 2019, 11 (1): 16-33.
- [36] Zhang Q Y, Mei L, Cao X H, Tang Y X, Zeng Z Y. Intercalation and exfoliation chemistries of transition metal dichalcogenides[J]. *J. Mater. Chem. A*, 2020, 8(31): 15417-15444.
- [37] Yang S, Zhang P P, Nia A S, Feng X L. Emerging 2D materials produced via electrochemistry[J]. *Adv. Mater.*, 2020, 32(10): 1907857.
- [38] Liu F M, Zhang L, Wang L, Cheng F Y. The electrochemical tuning of transition metal-based materials for electrocatalysis[J]. *Electrochem. Energy Rev.*, 2021, 4(1): 146-168.
- [39] Baumgärtner M E, Raub C J. The electrodeposition of platinum and platinum alloys[J]. *Platin. Met. Rev.*, 1988, 32(4): 188-197.
- [40] Ring L, Pollet B G, Chatenet M, Abbou S, Küpper K, Schmidt M, Huck M, Gries A, Steinhart M, Schäfer H. From bad electrochemical practices to an environmental and waste reducing approach for the generation of active hydrogen evolving electrodes[J]. *Angew. Chem. Int. Ed.*, 2019, 58(48): 17383-17392.
- [41] Yang F Z, Xu S K, Yao S B, Chen B Y, Zheng X Q, Zhong X H, Zhou S M. A study on the electrodeposition of palladium and its nucleation[J]. *J. Electrochem.*, 1997, (1): 103-108.
- [42] Edison T N J I, Atchudan R, Karthik N, Chandrasekaran S, Perumal S, Raja P B, Perumal V, Lee Y R. Deep eutectic solvent assisted electrosynthesis of ruthenium nanoparticles on stainless steel mesh for electrocatalytic hydrogen evolution reaction[J]. *Fuel*, 2021, 297: 120786.
- [43] Wang S J, Zou X L, Lu Y, Rao S C, Xie X L, Pang Z Y, Lu X G, Xu Q, Zhou Z F. Electrodeposition of nano-nickel in deep eutectic solvents for hydrogen evolution reaction in alkaline solution[J]. *Int. J. Hydrog. Energy*, 2018, 43(33): 15673-15686.
- [44] Smith E L, Abbott A P, Ryder K S. Deep eutectic solvents (DESs) and their applications[J]. *Chem. Rev.*, 2014, 114(21): 11060-11082.
- [45] Zhou M, Dick J E, Bard A J. Electrodeposition of isolated platinum atoms and clusters on bismuth-characterization and electrocatalysis[J]. *J. Am. Chem. Soc.*, 2017, 139 (48): 17677-17682.
- [46] Zhou M, Bao S J, Bard A J. Probing size and substrate effects on the hydrogen evolution reaction by single isolated Pt atoms, atomic clusters, and nanoparticles[J]. *J. Am. Chem. Soc.*, 2019, 141(18): 7327-7332.
- [47] Stanca S E, Vogt O, Zieger G, Ihring A, Dellith J, Undisz A, Rettenmayr M, Schmidt H. Electrochemical growth mechanism of nanoporous platinum layers[J]. *Commun. Chem.*, 2021, 4(1): 98.
- [48] Dehcheshmeh M S, Kiani A. Synthesis of Pt nano catalyst in the presence of carbon monoxide: superior activity towards hydrogen evolution reaction[J]. *Int. J. Hydrog. Energy*, 2019, 44(43): 23969-23974.
- [49] Cheng H E, Li W L, Yang Z P. Enhancement of hydrogen evolution reaction by Pt nanopillar-array electrode in alkaline media and the effect of nanopillar length on the electrode efficiency[J]. *Int. J. Hydrog. Energy*, 2019, 44 (57): 30141-30150.
- [50] Brimaud S, Behm R J. Electrodeposition of a Pt monolayer film: Using kinetic limitations for atomic layer epitaxy [J]. *J. Am. Chem. Soc.*, 2013, 135(32): 11716-11719.
- [51] Chen X X, Li N, Eckhard K, Stoica L, Xia W, Assmann J, Muhler M, Schuhmann W. Pulsed electrodeposition of Pt nanoclusters on carbon nanotubes modified carbon materials using diffusion restricting viscous electrolytes [J]. *Electrochem. Commun.*, 2007, 9(6): 1348-1354.
- [52] Hussein H E M, Maurer R J, Amari H, Peters J J P, Meng L C, Beanland R, Newton M E, Macpherson J V. Tracking metal electrodeposition dynamics from nucleation and growth of a single atom to a crystalline nanoparticle [J]. *ACS Nano*, 2018, 12(7): 7388-7396.
- [53] Huang K, Shin K, Henkelman G, Crooks R M. Correlating surface structures and electrochemical activity using shape-controlled single-Pt nanoparticles[J]. *ACS Nano*, 2021, 15(11): 17926-17937.
- [54] Glasscott M W, Dick J E. Fine-tuning porosity and time-resolved observation of the nucleation and growth of single platinum nanoparticles[J]. *ACS Nano*, 2019, 13 (4): 4572-4581.
- [55] Ye F, Li J J, Wang T T, Liu Y, Wei H J, Li J L, Wang X

- D. Electrocatalytic properties of platinum catalysts prepared by pulse electrodeposition method using  $\text{SnO}_2$  as an assisting reagent[J]. *J. Phys. Chem. C*, 2008, 112(33): 12894-12898.
- [56] Ohyama J, Sato T, Yamamoto Y, Arai S, Satsuma A. Size specifically high activity of Ru nanoparticles for hydrogen oxidation reaction in alkaline electrolyte[J]. *J. Am. Chem. Soc.*, 2013, 135(21): 8016-8021.
- [57] He Y P, Sheng Q L, Zheng J B. Double-template electrosynthesis of platinum nanomaterials for sensing application[J]. *Sens. Actuators B Chem.*, 2012, 166: 89-96.
- [58] Li Y J, Zhang H C, Xu T H, Lu Z Y, Wu X C, Wan P B, Sun X M, Jiang L. Under-water superacrophobic pine-shaped Pt nanoarray electrode for ultrahigh-performance hydrogen evolution[J]. *Adv. Funct. Mater.*, 2015, 25(11): 1737-1744.
- [59] Tavakkoli M, Holmberg N, Kronberg R, Jiang H, Sainio J, Kauppinen E I, Kallio T, Laasonen K. Electrochemical activation of single-walled carbon nanotubes with pseudo-atomic-scale platinum for the hydrogen evolution reaction[J]. *ACS Catal.*, 2017, 7(5): 3121-3130.
- [60] Dudin P V, Snowden M E, Macpherson J V, Unwin P R. Electrochemistry at nanoscale electrodes: Individual single-walled carbon nanotubes (SWNTs) and SWNT-templated metal nanowires[J]. *ACS Nano*, 2011, 5(12): 10017-10025.
- [61] Ye S H, Luo F Y, Zhang Q L, Zhang P Y, Xu T T, Wang Q, He D S, Guo L C, Zhang Y, He C X, Ouyang X P, Gu M, Liu J H, Sun X L. Highly stable single Pt atomic sites anchored on aniline-stacked graphene for hydrogen evolution reaction[J]. *Energy Environ. Sci.*, 2019, 12(3): 1000-1007.
- [62] Xu G R, Hui J J, Huang T, Chen Y, Lee J M. Platinum nanocuboids supported on reduced graphene oxide as efficient electrocatalyst for the hydrogen evolution reaction[J]. *J. Power Sources*, 2015, 285: 393-399.
- [63] Zhang H B, An P F, Zhou W, Guan B Y, Zhang P, Dong J C, Lou X W D. Dynamic traction of latticeconfined platinum atoms into mesoporous carbon matrix for hydrogen evolution reaction[J]. *Sci. Adv.*, 2018, 4(1): eaao-6657.
- [64] Wang Y H, Chen L, Yu X M, Wang Y G, Zheng G F. Superb alkaline hydrogen evolution and simultaneous electricity generation by Pt-decorated  $\text{Ni}_3\text{N}$  nanosheets[J]. *Adv. Energy Mater.*, 2017, 7(2): 1601390.
- [65] Bose C S C, Rajeshwar K. Efficient electrocatalyst as ssemblies for proton and oxygen reduction: The electrosynthesis and characterization of polypyrrole films containing nanodispersed platinum particles[J]. *J. Electroanal. Chem.*, 1992, 333(1-2): 235-256.
- [66] Zhou C F, Liu Z W, Yan Y S, Du X S, Mai Y W, Ringer S. Electro-synthesis of novel nanostructured pedot films and their application as catalyst support[J]. *Nanoscale Res. Lett.*, 2011, 6: 364.
- [67] Nieminen J J, Hatay I, Ge P Y, Méndez M A, Murtomäki L, Girault H H. Hydrogen evolution catalyzed by electrodeposited nanoparticles at the liquid/liquid interface[J]. *Chem. Commun.*, 2011, 47(19): 5548-5550.
- [68] Aslan E, Patir I H, Ersoz M. Cu nanoparticles electrodeposited at liquid-liquid interfaces: A highly efficient catalyst for the hydrogen evolution reaction[J]. *Chem. Eur. J.*, 2015, 21(12): 4585-4589.
- [69] Xiao H, Zhang J J, Zhao M, Ma J C, Li Y, Hu T J, Zheng Z F, Jia J F, Wu H S. Electric field-assisted synthesis of Pt, carbon quantum dots-coloaded graphene hybrid for hydrogen evolution reaction[J]. *J. Power Sources*, 2020, 451: 227770.
- [70] Xiao H, Xue S F, Zhang J J, Zhao M, Ma J C, Chen S, Zheng Z F, Jia J F, Wu H S. Facile electrolytic synthesis of Pt and carbon quantum dots coloaded multiwall carbon nanotube as highly efficient electrocatalyst for hydrogen evolution and ethanol oxidation[J]. *Chem. Eng. J.*, 2021, 408: 127271.
- [71] Liu L, Wang Y, Zhao Y Z, Wang Y, Zhang Z L, Wu T, Qin W J, Liu S J, Jia B R, Wu H Y, Zhang D Y, Qu X H, Chhowalla M, Qin M L. Ultrahigh Pt-mass-activity hydrogen evolution catalyst electrodeposited from bulk Pt[J]. *Adv. Funct. Mater.*, 2022, 32(20): 2112207.
- [72] Cao Z M, Chen Q L, Zhang J W, Li H Q, Jiang Y Q, Shen S Y, Fu G, Lu B A, Xie Z X, Zheng L S. Platinum-nickel alloy excavated nano-multipods with hexagonal close-packed structure and superior activity towards hydrogen evolution reaction[J]. *Nat. Commun.*, 2017, 8: 15131.
- [73] Isarain-Chávez E, Baró M D, Alcantara C, Pané S, Sort J, Pellicer E. Micelle-assisted electrodeposition of mesoporous Fe-Pt smooth thin films and their electrocatalytic activity towards the hydrogen evolution reaction[J]. *ChemSusChem*, 2018, 11(2): 367-375.
- [74] Palaniappan R, Ingram D C, Botte G G. Hydrogen evolution reaction kinetics on electrodeposited Pt-M (M = Ir, Ru, Rh, and Ni) cathodes for ammonia electrolysis[J]. *J. Electrochem. Soc.*, 2014, 161(1): E12-E22.
- [75] Xu W, Du D W, Lan R, Humphreys J, Miller D N, Walker M, Wu Z C, Irvine J T S, Tao S W. Electrodeposited NiCu bimetal on carbon paper as stable non-noble anode for efficient electrooxidation of ammonia[J]. *App. Cat. B*

- Environ., 2018, 237: 1101-1109.
- [76] Cherevko S, Kulyk N, Chung C H. Nanoporous Pt@Au<sub>x</sub>-Cu<sub>100-x</sub> by hydrogen evolution assisted electrodeposition of Au<sub>x</sub>Cu<sub>100-x</sub> and galvanic replacement of Cu with Pt: Electrocatalytic properties[J]. *Langmuir*, 2012, 28(6): 3306-3315.
- [77] Eiler K, Suriñach S, Sort J, Pellicer E. Mesoporous Ni-rich Ni-Pt thin films: Electrodeposition, characterization and performance toward hydrogen evolution reaction in acidic media[J]. *Appl. Catal. B Environ.*, 2020, 265: 118597.
- [78] Xu L, Cao L L, Xu W, Pei Z H. One-step electrosynthesis of NiFe-NF electrodes for highly efficient overall water splitting[J]. *Appl. Surf. Sci.*, 2020, 503: 144122.
- [79] Glasscott M W, Pendergast A D, Goines S, Bishop A R, Hoang A T, Renault C, Dick J E. Electrosynthesis of high-entropy metallic glass nanoparticles for designer, multi-functional electrocatalysis[J]. *Nat. Commun.*, 2019, 10: 2650.
- [80] Lee J K, Yi Y, Lee H J, Uhm S, Lee J. Electrocatalytic activity of Ni nanowires prepared by galvanic electrodeposition for hydrogen evolution reaction[J]. *Catal. Today*, 2009, 146(1-2): 188-191.
- [81] Shao Q, Wang Y, Yang S Z, Lu K Y, Zhang Y, Tang C Y, Song J, Feng Y G, Xiong L K, Peng Y, Li Y F, Xin H L L, Huang X Q. Stabilizing and activating metastable nickel nanocrystals for highly efficient hydrogen evolution electrocatalysis[J]. *ACS Nano*, 2018, 12(11): 11625-11631.
- [82] Wen X D, Yang X Y, Li M, Bai L, Guan J Q. Co/CoO<sub>x</sub> nanoparticles inlaid onto nitrogen-doped carbon-graphene as a trifunctional electrocatalyst[J]. *Electrochim. Acta*, 2019, 296: 830-841.
- [83] Chang T Y, Zhang B H, Cong W B, Luo Y. Study on hydrogen evolution performance of nickel-tin electrode[J]. *J. Electrochem.*, 2002, (3): 343-347.
- [84] Lu S G, Li Q, Liu Q G, Lu C, Dang B, Yang H X. The hydrogen evolution reaction on the hydrogen storage alloy electrode[J]. *J. Electrochem.*, 1998, (3): 265-272.
- [85] Yu W Z, Ma J, Chu Y M, Zhu H Z, Wang H J, Liu S C. Hydrogen evolution reaction on nanocrystalline Co-Mo/Ni composite-coated electrodes[J]. *J. Electrochem.*, 1996, (1): 47-53.
- [86] Wu Z X, Wang J, Guo J P, Zhu J, Wang D L. Recent progresses in molybdenum-based electrocatalysts for the hydrogen evolution reaction[J]. *J. Electrochem.*, 2016, 22(2): 192-204.
- [87] Ding L, Li K, Xie Z Q, Yang G Q, Yu S L, Wang W T, Yu H R, Baxter J, Meyer H M, Cullen D A, Zhang F Y. Constructing ultrathin W-doped nife nanosheets via facile electrosynthesis as bifunctional electrocatalysts for efficient water splitting[J]. *ACS Appl. Mater. Interfaces*, 2021, 13(17): 20070-20080.
- [88] Zhang L, Liu B R, Zhang N, Ma M M. Electrosynthesis of Co<sub>3</sub>O<sub>4</sub> and Co(OH)<sub>2</sub> ultrathin nanosheet arrays for efficient electrocatalytic water splitting in alkaline and neutral media[J]. *Nano Res.*, 2018, 11(1): 323-333.
- [89] Xiao P, Sk M A, Thia L, Ge X M, Lim R J, Wang J Y, Lim K H, Wang X. Molybdenum phosphide as an efficient electrocatalyst for the hydrogen evolution reaction [J]. *Energy Environ. Sci.*, 2014, 7(8): 2624-2629.
- [90] Lu Z P, Sepunaru L. Electrodeposition of iron phosphide film for hydrogen evolution reaction[J]. *Electrochim. Acta*, 2020, 363: 137167.
- [91] Xing J H, Li H, Cheng M M C, Geyer S M, Ng K Y S. Electro-synthesis of 3D porous hierarchical Ni-Fe phosphate film/Ni foam as a high-efficiency bifunctional electrocatalyst for overall water splitting[J]. *J. Mater. Chem. A*, 2016, 4(36): 13866-13873.
- [92] Chen M X, Qi J, Zhang W, Cao R. Electrosynthesis of NiP<sub>x</sub> nanospheres for electrocatalytic hydrogen evolution from a neutral aqueous solution[J]. *Chem. Commun.*, 2017, 53(40): 5507-5510.
- [93] Lin C Y, Huang S C, Lin Y G, Hsu L C, Yi C T. Electrosynthesized Ni-P nanospheres with high activity and selectivity towards photoelectrochemical plastics reforming[J]. *Appl. Catal. B Environ.*, 2021, 296: 120351.
- [94] Jiang N, You B, Sheng M L, Sun Y J. Electrodeposited cobalt-phosphorous-derived films as competent bifunctional catalysts for overall water splitting[J]. *Angew. Chem. Int. Ed.*, 2015, 54(21): 6251-6254.
- [95] Jiang N, You B, Boonstra R, Rodriguez I M T, Sun Y J. Integrating electrocatalytic 5-hydroxymethylfurfural oxidation and hydrogen production via Co-P-derived electrocatalysts[J]. *ACS Energy Lett.*, 2016, 1(2): 386-390.
- [96] Aliyev A S, Elrouby M, Cafarova S F. Electrochemical synthesis of molybdenum sulfide semiconductor[J]. *Mater. Sci. Semicond. Process.*, 2015, 32: 31-39.
- [97] Gopalakrishnan D, Damien D, Li B, Gullappalli H, Pillai V K, Ajayan P M, Shaijumon M M. Electrochemical synthesis of luminescent MoS<sub>2</sub> quantum dots[J]. *Chem. Commun.*, 2015, 51(29): 6293-6296.
- [98] Cao Y. Roadmap and direction toward high-performance MoS<sub>2</sub> hydrogen evolution catalysts[J]. *ACS Nano*, 2021, 15(7): 11014-11039.
- [99] Murugesan S, Akkineni A, Chou B P, Glaz M S, Bout D A V, Stevenson K J. Room temperature electrodeposition

- of molybdenum sulfide for catalytic and photoluminescence applications[J]. *ACS Nano*, 2013, 7(9): 8199-8205.
- [100] Gao Y, Zhou J, Liu Y W, Chen S L. Hydrogen evolution properties on individual MoS<sub>2</sub> nanosheets[J]. *J. Electrochem.*, 2016, 22(6): 590-595.
- [101] Tan S M, Pumera M. Bottom-up electrosynthesis of highly active tungsten sulfide (WS<sub>3x</sub>) films for hydrogen evolution[J]. *ACS Appl. Mater. Interfaces*, 2016, 8(6): 3948-3957.
- [102] Tan S M, Pumera M. Electrosynthesis of bifunctional WS<sub>3x</sub>/reduced graphene oxide hybrid for hydrogen evolution reaction and oxygen reduction reaction electrocatalysis[J]. *Chem. Euro. J.*, 2017, 23(35): 8510-8519.
- [103] Jo S, Lee K B, Sohn J I. Direct electrosynthesis of selective transition-metal chalcogenides as functional catalysts with a tunable activity for efficient water electrolysis[J]. *ACS Sustain. Chem. Eng.*, 2021, 9(44): 14911-14917.
- [104] Chen W S, Gu J J, Liu Q L, Yang M Z, Zhan C, Zang X N, Pham T A, Liu G X, Zhang W, Zhang D, Dunn B, Wang Y M. Two-dimensional quantum-sheet films with sub-1.2 nm channels for ultrahigh-rate electrochemical capacitance[J]. *Nat. Nanotechnol.*, 2022, 17(2): 153-158.
- [105] Wang H T, Lu Z Y, Kong D S, Sun J, Hymel T M, Cui Y. Electrochemical tuning of MoS<sub>2</sub> nanoparticles on three-dimensional substrate for efficient hydrogen evolution[J]. *ACS Nano*, 2014, 8(5): 4940-4947.
- [106] Michalsky R, Zhang Y J, Peterson A A. Trends in the hydrogen evolution activity of metal carbide catalysts [J]. *ACS Catal.*, 2014, 4(5): 1274-1278.
- [107] Fan X J, Peng Z W, Ye R Q, Zhou H Q, Guo X. M3C (M: Fe, Co, Ni) nanocrystals encased in graphene nanoribbons: An active and stable bifunctional electrocatalyst for oxygen reduction and hydrogen evolution reactions[J]. *ACS Nano*, 2015, 9(7): 7407-7418.
- [108] Jiang R, Fan J H, Hu L Y, Dou Y P, Mao X H, Wang D H. Electrochemically synthesized N-doped molybdenum carbide nanoparticles for efficient catalysis of hydrogen evolution reaction[J]. *Electrochim. Acta*, 2018, 261: 578-587.
- [109] Fan J H, Dou Y P, Jiang R, Du K F, Deng B W, Wang D H. Electro-synthesis of tungsten carbide containing catalysts in molten salt for efficiently electrolytic hydrogen generation assisted by urea oxidation[J]. *Int. J. Hydrog. Energy*, 2021, 46(28): 14932-14943.
- [110] Malakzadeh M, Raoof J B, Ghafarnejad A, Ojani R. *In-situ* electrosynthesis Cu-PtBTC MOF-derived nanocomposite modified glassy carbon electrode for highly performance electrocatalysis of hydrogen evolution reaction[J]. *J. Electroanal. Chem.*, 2021, 900: 115716.
- [111] Varsha M V, Nageswaran G. Review—direct electrochemical synthesis of metal organic frameworks[J]. *J. Electrochem. Soc.*, 2020, 167(15): 155527.
- [112] Babar P T, Lokhande A C, Jo E, Pawar B S, Gang M G, Pawar S M, Kim J H. Facile electrosynthesis of Fe (Ni/Co) hydroxyphosphate as a bifunctional electrocatalyst for efficient water splitting[J]. *J. Ind. Eng. Chem.*, 2019, 70: 116-123.
- [113] Liu L, Hai Y, Gong Y. A facile electrosynthesis of terephthalate (tp)-based metal-organic framework, Ni<sub>3</sub>(OH)<sub>2</sub>(H<sub>2</sub>O)<sub>2</sub>(tp)<sub>2</sub> with superior catalytic activity for hydrogen evolution reaction[J]. *Eur. J. Inorg. Chem.*, 2020, 2020(44): 4215-4224.
- [114] Liberman I, Ifraimov R, Shimon R, Hod I. Localized electrosynthesis and subsequent electrochemical mapping of catalytically active metal-organic frameworks [J]. *Adv. Funct. Mater.*, 2022, 32(19): 2112517.
- [115] Zhou K L, Wang Z L, Han C B, Ke X X, Wang C H, Jin Y H, Zhang Q Q, Liu J B, Wang H, Yan H. Platinum single-atom catalyst coupled with transition metal/metal oxide heterostructure for accelerating alkaline hydrogen evolution reaction[J]. *Nat. Commun.*, 2021, 12(1): 3783.
- [116] Tiwari J N, Sultan S, Myung C W, Yoon T, Li N N, Ha M R, Harzandi A M, Park H J, Kim D Y, Chandrasekaran S S, Lee W G, Vij V, Kang H J, Shin T J, Shin H S, Lee G, Lee Z, Kim K S. Multicomponent electrocatalyst with ultralow Pt loading and high hydrogen evolution activity[J]. *Nat. Energy*, 2018, 3(9): 773-782.
- [117] Chia X Y, Sutrisnoh N A A, Pumera M. Tunable Pt-MoS<sub>2</sub> hybrid catalysts for hydrogen evolution [J]. *ACS Appl. Mater. Interfaces*, 2018, 10(10): 8702-8711.
- [118] Jiang R, Deng B W, Pi L, Hu L Y, Chen D, Dou Y P, Mao X H, Wang D H. Molten electrolyte-modulated electrosynthesis of multi-anion Mo-based lamellar nanohybrids derived from natural minerals for boosting hydrogen evolution[J]. *ACS Appl. Mater. Interfaces*, 2020, 12(52): 57870-57880.
- [119] Song F Z, Li W, Han G Q, Sun Y J. Electropolymerization of aniline on nickel-based electrocatalysts substantially enhances their performance for hydrogen evolution[J]. *ACS Appl. Energy Mater.*, 2018, 1(1): 3-8.
- [120] Chen Z F, Ye S R, Wilson A R, Ha Y C, Wiley B J. Optically transparent hydrogen evolution catalysts made from networks of copper-platinum core-shell nanowires [J]. *Energy Environ. Sci.*, 2014, 7(4): 1461-1467.
- [121] Subbaraman R, Tripkovic D, Strmcnik D, Chang K C,

- Uchimura M, Paulikas A P, Stamenkovic V, Markovic N M. Enhancing hydrogen evolution activity in water splitting by tailoring  $\text{Li}^+\text{-Ni(OH)}_2\text{-Pt}$  interfaces[J]. *Science*, 2011, 334(6060): 1256-1260.
- [122] Li L, Wang B, Zhang G W, Yang G, Yang T, Yang S, Yang S C. Electrochemically modifying the electronic structure of  $\text{IrO}_2$  nanoparticles for overall electrochemical water splitting with extensive adaptability[J]. *Adv. Energy Mater.*, 2020, 10(30): 2001600.
- [123] Park J, Kim H, Jin K, Lee B J, Park Y S, Kim H, Park I, Yang K D, Jeong H Y, Kim J, Hong K T, Jang H W, Kang K, Nam K T. A new water oxidation catalyst: lithium manganese pyrophosphate with tunable Mn valency[J]. *J. Am. Chem. Soc.*, 2014, 136(11): 4201-4211.
- [124] Wang H T, Lu Z Y, Xu S C, Kong D S, Cha J J, Zheng G Y, Hsu P C, Yan K, Bradshaw D, Prinz F B, Cui Y. Electrochemical tuning of vertically aligned  $\text{MoS}_2$  nanofilms and its application in improving hydrogen evolution reaction[J]. *Proc. Natl. Acad. Sci. U.S.A.*, 2013, 110(49): 19701-19706.
- [125] Meng J, Liu F M, Yan Z H, Cheng F Y, Li F J, Chen J. Spent alkaline battery-derived manganese oxides as efficient oxygen electrocatalysts for Zn-air batteries [J]. *Inorg. Chem. Front.*, 2018, 5(9): 2167-2173.
- [126] Wang H T, Xu S C, Tsai C, Li Y Z, Liu C, Zhao J, Liu Y Y, Yuan H Y, Abild-Pedersen F, Prinz F B, Nørskov J K, Cui Y. Direct and continuous strain control of catalysts with tunable battery electrode materials[J]. *Science*, 2016, 354(6315): 1031-1036.
- [127] Tang C, Zhang R, Lu W B, Wang Z, Liu D N, Hao S, Du G, Asiri A M, Sun X P. Energy-saving electrolytic hydrogen generation:  $\text{Ni}_2\text{P}$  nanoarray as a high-performance non-noble-metal electrocatalyst[J]. *Angew. Chem. Int. Ed.*, 2017, 56(3): 842-846.
- [128] Liu H, Liu Y, Li M, Liu X, Luo J. Transition-metal-based electrocatalysts for hydrazine-assisted hydrogen production[J]. *Mater. Today Adv.*, 2020, 7: 100083.
- [129] Wang J M, Ma X, Liu T T, Liu D N, Hao S, Du G, Kong R M, Asiri A M, Sun X P.  $\text{NiS}_2$  nanosheet array: A high-active bifunctional electrocatalyst for hydrazine oxidation and water reduction toward energy-efficient hydrogen production[J]. *Mater. Today Energy*, 2017, 3: 9-14.
- [130] Zhang J Y, Wang H M, Tian Y F, Yan Y, Xue Q, He T, Liu H F, Wang C D, Chen Y, Xia B Y. Anodic hydrazine oxidation assists energy-efficient hydrogen evolution over a bifunctional cobalt perselenide nanosheet electrode[J]. *Angew. Chem. Int. Ed.*, 2018, 57(26): 7649-7653.
- [131] Li Y P, Zhang J H, Liu Y, Qian Q Z, Li Z Y, Zhu Y, Zhang G Q. Partially exposed  $\text{RuP}_2$  surface in hybrid structure endows its bifunctionality for hydrazine oxidation and hydrogen evolution catalysis[J]. *Sci. Adv.*, 2020, 6(44): eabb4197.
- [132] Qian Q Z, Zhang J H, Li J M, Li Y P, Jin X, Zhu Y, Liu Y, Li Z Y, El-Harairy A, Xiao C, Zhang G Q, Xie Y. Artificial heterointerfaces achieve delicate reaction kinetics towards hydrogen evolution and hydrazine oxidation catalysis[J]. *Angew. Chem. Int. Ed.*, 2021, 60(11): 5984-5993.
- [133] Liu Y, Zhang J H, Li Y P, Qian Q Z, Li Z Y, Zhang G Q. Realizing the synergy of interface engineering and chemical substitution for  $\text{Ni}_3\text{N}$  enables its bifunctionality toward hydrazine oxidation assisted energy-saving hydrogen production[J]. *Adv. Funct. Mater.*, 2021, 31(35): 2103673.
- [134] Wang Z Y, Xu L, Huang F Z, Qu L B, Li J T, Owusu K A, Liu Z, Lin Z F, Xiang B H, Liu X, Zhao K N, Liao X B, Yang W, Cheng Y B, Mai L Q. Copper-nickel nitride nanosheets as efficient bifunctional catalysts for hydrazine-assisted electrolytic hydrogen production[J]. *Adv. Energy Mater.*, 2019, 9(21): 1900390.
- [135] Sun F, Qin J S, Wang Z Y, Yu M Z, Wu X H, Sun X M, Qiu J S. Energy-saving hydrogen production by chlorine-free hybrid seawater splitting coupling hydrazine degradation[J]. *Nat. Commun.*, 2021, 12(1): 4182.
- [136] Yu Q P, Chi J Q, Liu G S, Wang X Y, Liu X B, Li Z J, Deng Y, Wang X P, Wang L. Dual-strategy of hetero-engineering and cation doping to boost energy-saving hydrogen production via hydrazine-assisted seawater electrolysis[J]. *Sci. China Mater.*, 2022, 65(6): 1539-1549.
- [137] Yu Z P, Xu J Y, Meng L J, Liu L F. Efficient hydrogen production by saline water electrolysis at high current densities without the interfering chlorine evolution[J]. *J. Mater. Chem. A*, 2021, 9(39): 22248-22253.
- [138] Deng K, Mao Q Q, Wang W X, Wang P, Wang Z Q, Xu Y, Li X N, Wang H J, Wang L. Defect-rich low-crystalline Rh metallene for efficient chlorine-free  $\text{H}_2$  production by hydrazine-assisted seawater splitting[J]. *App. Catal. B Environ.*, 2022, 310: 121338.
- [139] Liu Y, Zhang J H, Li Y P, Qian Q Z, Li Z Y, Zhu Y, Zhang G Q. Manipulating dehydrogenation kinetics through dual-doping  $\text{Co}_3\text{N}$  electrode enables highly efficient hydrazine oxidation assisting self-powered  $\text{H}_2$  production[J]. *Nat. Commun.*, 2020, 11(1): 1853.

- [140] Liu X J, He J, Zhao S Z, Liu Y P, Zhao Z, Luo J, Hu G Z, Sun X M, Ding Y. Self-powered H<sub>2</sub> production with bifunctional hydrazine as sole consumable[J]. *Nat. Commun.*, 2018, 9: 4365.
- [141] Liu T T, Liu D N, Qu F L, Wang D X, Zhang L, Ge R X, Hao S, Ma Y J, Du G, Asiri A M, Chen L, Sun X P. Enhanced electrocatalysis for energy-efficient hydrogen production over CoP catalyst with nonelectroactive Zn as a promoter[J]. *Adv. Energy Mater.*, 2017, 7(15): 1700020.
- [142] Yu Z Y, Lang C C, Gao M R, Chen Y, Fu Q Q, Duan Y, Yu S H. Ni-Mo-O nanorod-derived composite catalysts for efficient alkaline water-to-hydrogen conversion via urea electrolysis[J]. *Energy Environ. Sci.*, 2018, 11(7): 1890-1897.
- [143] Zhang L S, Wang L P, Lin H P, Liu Y X, Ye J Y, Wen Y Z, Chen A, Wang L, Ni F L, Zhou Z Y, Sun S G, Li Y Y, Zhang B, Peng H S. A lattice-oxygen-involved reaction pathway to boost urea oxidation[J]. *Angew. Chem. Int. Ed.*, 2019, 58(47): 16820-16825.
- [144] Wang C, Lu H L, Mao Z Y, Yan C L, Shen G Z, Wang X F. Bimetal schottky heterojunction boosting energy-saving hydrogen production from alkaline water via urea electrocatalysis[J]. *Adv. Funct. Mater.*, 2020, 30(21): 20000556.
- [145] Hu S N, Wang S Q, Feng C Q, Wu H M, Zhang J J, Mei H. Novel MOF-derived nickel nitride as high-performance bifunctional electrocatalysts for hydrogen evolution and urea oxidation[J]. *ACS Sustainable Chem. Eng.*, 2020, 8(19): 7414-7422.
- [146] Chen N, Du Y X, Zhang G, Lu W T, Cao F F. Amorphous nickel sulfoselenide for efficient electrochemical urea-assisted hydrogen production in alkaline media[J]. *Nano Energy*, 2021, 81: 105605.
- [147] Xu W, Lan R, Du D W, Humphreys J, Walker M, Wu Z C, Wang H T, Tao S W. Directly growing hierarchical nickel-copper hydroxide nanowires on carbon fibre cloth for efficient electrooxidation of ammonia[J]. *App. Cat. B Environ.*, 2017, 218: 470-479.
- [148] Wu F C, Ou G, Yang J, Li H N, Gao Y X, Chen F M, Wang Y, Shi Y M. Bifunctional nickel oxide-based nanosheets for highly efficient overall urea splitting[J]. *Chem. Commun.*, 2019, 55(46): 6555-6558.
- [149] Xu Q L, Qian G F, Yin S B, Yu C, Chen W, Yu T Q, Luo L, Xia Y J, Tsiakaras P. Design and synthesis of highly performing bifunctional Ni-NiO-MoNi hybrid catalysts for enhanced urea oxidation and hydrogen evolution reactions[J]. *ACS Sustainable Chem. Eng.*, 2020, 8(18): 7174-7181.
- [150] Wu Y T, Wang H, Ren J W, Xu X, Wang X Y, Wang R F. Electrocatalyst based on Ni<sub>2</sub>P nanoparticles and NiCoP nanosheets for efficient hydrogen evolution from urea wastewater[J]. *J. Colloid Interface Sci.*, 2022, 608: 2932-2941.
- [151] Sacré N, Duca M, Garbarino S, Imbeault R, Wang A, Youssef A H, Galipaud J, Hufnagel G, Ruediger A, Roué L, Guay D. Tuning Pt-Ir interactions for NH<sub>3</sub> electrocatalysis[J]. *ACS Catal.*, 2018, 8(3): 2508-2518.
- [152] Zhou Y F, Zhang G Q, Yu M C, Wang X J, Lv J L, Yang F L. Free-standing 3D porous N-doped graphene aerogel supported platinum nanocluster for efficient hydrogen production from ammonia electrolysis[J]. *ACS Sustain. Chem. Eng.*, 2018, 6(7): 8437-8446.
- [153] Gwak J, Choun M, Lee J. Alkaline ammonia electrolysis on electrodeposited platinum for controllable hydrogen production[J]. *ChemSusChem*, 2016, 9(4): 403-408.
- [154] Sun H Y, Xu G R, Li F M, Hong Q L, Jin P J, Chen P, Chen Y. Hydrogen generation from ammonia electrolysis on bifunctional platinum nanocubes electrocatalysts [J]. *J. Energy Chem.*, 2020, 47: 234-240.
- [155] Xue Q, Zhao Y, Zhu J Y, Ding Y, Wang T J, Sun H Y, Li F M, Chen P, Jin P J, Yin S B, Chen Y. PtRu nanocubes as bifunctional electrocatalysts for ammonia electrolysis[J]. *J. Mater. Chem. A*, 2021, 9(13): 8444-8451.
- [156] Shilpa N, Pandikassala A, Krishnaraj P, Walko P S, Devi R N, Kurungot S. Co-Ni layered double hydroxide for the electrocatalytic oxidation of organic molecules: An approach to lowering the overall cell voltage for the water splitting process[J]. *ACS Appl. Mater. Interfaces*, 2022, 14(14): 16222-16232.
- [157] Wei J C, Shi L, Wu X. Simultaneous hydrogen and (NH<sub>4</sub>)<sub>2</sub>SO<sub>4</sub> productions from desulfurization wastewater electrolysis using MEA electrolyser[J]. *J. Electrochem.*, 2022, 28(5): 4-12.
- [158] Miller H A, Lavacchi A, Vizza F. Storage of renewable energy in fuels and chemicals through electrochemical reforming of bioalcohols[J]. *Curr. Opin. Electrochem.*, 2020, 21: 140-145.
- [159] Arshad F, Ul-Haq T, Hiussain I, Sher F. Recent advances in electrocatalysts toward alcohol-assisted, energy-saving hydrogen production[J]. *ACS Appl. Mater. Interfaces*, 2021, 4(9): 8685-8701.
- [160] Coutanceau C, Baranton S. Electrochemical conversion of alcohols for hydrogen production: A short overview [J]. *WIREs Energy Environ.*, 2016, 5(4): 388-400.

- [161] Wu T X, Zhu X G, Wang G Z, Zhang Y X, Zhang H M, Zhao H J. Vapor-phase hydrothermal growth of single crystalline NiS<sub>2</sub> nanostructure film on carbon fiber cloth for electrocatalytic oxidation of alcohols to ketones and simultaneous H<sub>2</sub> evolution[J]. *Nano Res.*, 2018, 11(2): 1004-1017.
- [162] Bambagioni V, Bevilacqua M, Bianchini C, Filippi J, Lavacchi A, Marchionni A, Vizza F, Shen P K. Self-sustainable production of hydrogen, chemicals, and energy from renewable alcohols by electrocatalysis[J]. *ChemSusChem*, 2010, 3(7): 851-855.
- [163] Chen Y X, Lavacchi A, Miller H A, Bevilacqua M, Filippi J, Innocenti M, Marchionni A, Oberhauser W, Wang L, Vizza F. Nanotechnology makes biomass electrolysis more energy efficient than water electrolysis[J]. *Nat. Commun.*, 2014, 5: 4036.
- [164] Miller H A, Bellini M, Vizza F, Hasenöhrl C, Tilley R D. Carbon supported Au-Pd core-shell nanoparticles for hydrogen production by alcohol electroreforming [J]. *Catal. Sci. Technol.*, 2016, 6(18): 6870-6878.
- [165] Zhao X J, Dai L, Qin Q, Pei F, Hu C Y, Zheng N F. Self-supported 3D PdCu alloy nanosheets as a bifunctional catalyst for electrochemical reforming of ethanol [J]. *Small*, 2017, 13(12): 1602970.
- [166] Dai L, Qin Q, Zhao X J, Xu C F, Hu C Y, Mo S G, Wang Y O, Lin S C, Tang Z C, Zheng N F. Electrochemical partial reforming of ethanol into ethyl acetate using ultrathin Co<sub>3</sub>O<sub>4</sub> nanosheets as a highly selective anode catalyst[J]. *ACS Cent. Sci.*, 2016, 2(8): 538-544.
- [167] Zhou C H C, Beltramini J N, Fan Y X, Lu G Q M. Chemoselective catalytic conversion of glycerol as a biorenewable source to valuable commodity chemicals [J]. *Chem. Soc. Rev.*, 2008, 37(3): 527-549.
- [168] Lam C H, Bloomfield A J, Anastas P T. A switchable route to valuable commodity chemicals from glycerol via electrocatalytic oxidation with an earth abundant metal oxidation catalyst[J]. *Green Chem.*, 2017, 19(8): 1958-1968.
- [169] Li Y, Wei X F, Chen L S, Shi J L, He M Y. Nickel-molybdenum nitride nanoplate electrocatalysts for concurrent electrolytic hydrogen and formate productions [J]. *Nat. Commun.*, 2019, 10: 5335.
- [170] Zheng J, Chen X L, Zhong X, Li S Q, Liu T Z, Zhuang G L, Li X N, Deng S W, Mei D H, Wang J G. Hierarchical porous NC@CuCo nitride nanosheet networks: Highly efficient bifunctional electrocatalyst for overall water splitting and selective electrooxidation of benzyl alcohol[J]. *Adv. Funct. Mater.*, 2017, 27(46): 1704169.
- [171] Si D, Xiong B Y, Chen L S, Shi J L. Highly selective and efficient electrocatalytic synthesis of glycolic acid in coupling with hydrogen evolution[J]. *Chem. Catal.*, 2021, 1(4): 941-955.
- [172] Liu W J, Xu Z R, Zhao D T, Pan X Q, Li H C, Hu X, Fan Z Y, Wang W K, Zhao G H, Jin S, Huber G W, Yu H Q. Efficient electrochemical production of glucaric acid and H<sub>2</sub> via glucose electrolysis[J]. *Nat. Commun.*, 2020, 11(1): 265.
- [173] Lin C, Zhang P J, Wang S Y, Zhou Q L, Na B, Li H Q, Tian J Y, Zhang Y, Deng C, Meng L Q, Wu J X, Liu C Z, Hu J Y, Zhang L M. Engineered porous Co-Ni alloy on carbon cloth as an efficient bifunctional electrocatalyst for glucose electrolysis in alkaline environment[J]. *J. Alloys Compd.*, 2020, 823: 153784.
- [174] Deng X H, Xu G Y, Zhang Y J, Wang L, Zhang J J, Li J F, Fu X Z, Luo J L. Understanding the roles of electro-generated Co<sup>3+</sup> and Co<sup>4+</sup> in selectivity-tuned 5-hydroxymethylfurfural oxidation[J]. *Angew. Chem. Int. Ed.*, 2021, 60(37): 20535-20542.
- [175] Huang Y, Chong X D, Liu C B, Liang Y, Zhang B. Boosting hydrogen production by anodic oxidation of primary amines over a NiSe nanorod electrode[J]. *Angew. Chem. Int. Ed.*, 2018, 57(40): 13163-13166.
- [176] Fu N K, Sauer G S, Saha A, Loo A, Lin S. Metal-catalyzed electrochemical diazidation of alkenes[J]. *Science*, 2017, 357(6351): 575-579.
- [177] Sauermann N, Mei R H, Ackermann L. Electrochemical C-H amination by cobalt catalysis in a renewable solvent[J]. *Angew. Chem. Int. Ed.*, 2018, 57(18): 5090-5094.
- [178] Wen Q L, Lin Y, Yang Y, Gao R J, Ouyang N Q, Ding D F, Liu Y W, Zhai T Y. *In situ* chalcogen leaching manipulates reactant interface toward efficient amine electrooxidation[J]. *ACS Nano*, 2022, 16(6): 9572-9582.
- [179] You B, Jiang N, Liu X, Sun Y J. Simultaneous H<sub>2</sub> generation and biomass upgrading in water by an efficient noble-metal-free bifunctional electrocatalyst[J]. *Angew. Chem. Int. Ed.*, 2016, 55(34): 9913-9917.
- [180] You B, Liu X, Jiang N, Sun Y J. A general strategy for decoupled hydrogen production from water splitting by integrating oxidative biomass valorization [J]. *J. Am. Chem. Soc.*, 2016, 138(41): 13639-13646.
- [181] Mika L T, Cséfalvay E, Németh A. Catalytic conversion of carbohydrates to initial platform chemicals: Chemistry and sustainability[J]. *Chem. Rev.*, 2018, 118(2): 505-613.
- [182] Zhang Z H, Huber G W. Catalytic oxidation of carbohydrates into organic acids and furan chemicals[J]. *Chem.*



- Soc. Rev., 2018, 47(4): 1351-1390.
- [183] Weber R S. Effective use of renewable electricity for making renewable fuels and chemicals[J]. *ACS Catal.*, 2019, 9(2): 946-950.
- [184] Pasta M, La Mantia F, Cui Y. Mechanism of glucose electrochemical oxidation on gold surface[J]. *Electrochim. Acta*, 2010, 55(20): 5561-5568.
- [185] Cui H F, Ye J S, Liu X, Zhang W D, Sheu F S. Pt-Pb alloy nanoparticle/carbon nanotube nanocomposite: A strong electrocatalyst for glucose oxidation[J]. *Nanotechnology*, 2006, 17(9): 2334-2339.
- [186] Zakrzewska M E, Bogel-Lukasik E, Bogel-Lukasik R. Ionic liquid-mediated formation of 5-hydroxymethylfurfural—a promising biomass-derived building block[J]. *Chem. Rev.*, 2011, 111(2): 397-417.
- [187] Moreau C, Belgacem M N, Gandini A. Recent catalytic advances in the chemistry of substituted furans from carbohydrates and in the ensuing polymers[J]. *Top. Catal.*, 2004, 27(1-4): 11-30.
- [188] Perry S C, Pangotra D, Vieira L, Csepei L I, Sieber V, Wang L, de León C P, Walsh F C. Electrochemical synthesis of hydrogen peroxide from water and oxygen[J]. *Nat. Rev. Chem.*, 2019, 3(7): 442-458.
- [189] Shi X J, Siahrostami S, Li G L, Zhang Y R, Chakthranont P, Studt F, Jaramillo T F, Zheng X L, Nørskov J K. Understanding activity trends in electrochemical water oxidation to form hydrogen peroxide[J]. *Nat. Commun.*, 2017, 8: 701.
- [190] Fuku K, Sayama K. Efficient oxidative hydrogen peroxide production and accumulation in photoelectrochemical water splitting using a tungsten trioxide/bismuth vanadate photoanode[J]. *Chem. Commun.*, 2016, 52(31): 5406-5409.
- [191] Kelly S R, Shi X J, Back S, Vallez L, Park S Y, Siahrostami S, Zheng X L, Nørskov J K. ZnO as an active and selective catalyst for electrochemical water oxidation to hydrogen peroxide[J]. *ACS Catal.*, 2019, 9(5): 4593-4599.
- [192] Izgorodin A, Izgorodina E, MacFarlane D R. Low overpotential water oxidation to hydrogen peroxide on a  $\text{MnO}_x$  catalyst[J]. *Energy Environ. Sci.*, 2012, 5(11): 9496-9501.
- [193] Wei J Q, Zhong L X, Xia H R, Lü Z S, Diao C Z, Zhang W, Li X, Du Y H, Xi S B, Salanne M, Chen X D, Li S Z. Metal-ion oligomerization inside electrified carbon micropores and its effect on capacitive charge storage[J]. *Adv. Mater.*, 2022, 34(4): 2107439.
- [194] Li Y H, Ozden A, Leow W R, Ou P F, Huang J N E, Wang Y H, Bertens K, Xu Y, Liu Y, Roy C, Jiang H, Sinton D, Li C Z, Sargent E H. Redox-mediated electrosynthesis of ethylene oxide from  $\text{CO}_2$  and water[J]. *Nat. Catal.*, 2022, 5(3): 185-192.
- [195] Wang Y T, Li T L, Yu Y F, Zhang B. Electrochemical synthesis of nitric acid from nitrogen oxidation[J]. *Angew. Chem. Int. Ed.*, 2022, 61(12): e202115409.
- [196] Guo Y, Zhang S C, Zhang R, Wang D H, Zhu D M, Wang X W, Xiao D W, Li N, Zhao Y W, Huang Z D, Xu W J, Chen S M, Song L, Fan J, Chen Q, Zhi C Y. Electrochemical nitrate production via nitrogen oxidation with atomically dispersed Fe on N-doped carbon nanosheets[J]. *ACS Nano*, 2021, 16(1): 655-663.
- [197] Jeanmairet G, Rotenberg B, Salanne M. Microscopic simulations of electrochemical double-layer capacitors[J]. *Chem. Rev.*, 2022, 122(12): 10860-10898.

# 电化学合成纳米材料和小分子材料在 电解制氢领域的应用

魏家祺, 陈晓东, 李述周\*

(南洋理工大学材料科学与工程学院, 新加坡 639798, 新加坡)

**摘要:** 氢气是一种清洁、高效、可再生的新型能源, 并且是未来碳中和能源供应中最具潜力的化石燃料替代品。因此, 可持续氢能源制造具有极大的吸引力与迫切的需求, 尤其是通过清洁、环保、零排放的电解水方法。然而, 目前的电解水反应受到其缓慢的动力学以及低成本/能源效率的制约。在这些方面, 电化学合成通过制造先进的电催化剂和提供更高效/增值的共电解替代品, 为提高水电解的效率和效益提供了广阔的前景。它是一种环保、简单的通过电解或其他电化学操作, 对从分子到纳米尺度的材料进行制造的方法。本文首先介绍了电化学合成的基本概念、设计方法以及常用方法。然后, 总结了电化学合成技术在电解水领域的应用及进展。我们专注于电化学合成的纳米结构电催化剂以实现更高效的电解水制氢, 以及小分子的电化学氧化以取代电解水制氢中的析氧共反应, 实现更高效、增值的共电解制氢。我们系统地讨论了电化学合成条件与产物的关系, 以启发未来的探索。最后, 本文讨论了电化学合成在先进电解水以及其他能量转换和储存应用方面的挑战和前景。

**关键词:** 电化学合成; 电解水; 电催化剂; 共电解; 有机电合成; 析氢反应